ebalanceplus

Report on algorithms to increase grid resilience at LV/MV level

Deliverable D4.2

Date: 2/2/2022
Author(s): Giamarelos Nikolaos, Mavromatakis Jason, Alifragkis Vagelis, Krzysztof Piotrowski

This project has received funding from the European Union's Horizon 2020 research and innovation programme under grand agreement N°864283

Technical References

Project Acronym	ebalance-plus
Project Title	Energy balancing and resilience solutions to unlock the flexibility and increase market options for distribution grid
Project Coordinator	CEMOSA
Project Duration	42 months

Deliverable No.	D4.2
Dissemination level [1]	PU
Work Package	WP4
Task	T4.2
Lead beneficiary	EMTECH
Contributing beneficiary(ies)	CEM, IHP, UMA, SOF, REE, TPS, MGC, UNC, JUN, DTU, ENF
Due date of deliverable	31 January 2022
Actual submission date	2 February 2022

[1] PU = Public
PP = Restricted to other programme participants (including the Commission Services)
RE = Restricted to a group specified by the consortium (including the Commission Services)
CO = Confidential, only for members of the consortium (including the Commission Services)

Document history

V	Date	Beneficiary(ies)	Author(s)
1	01.12.2021	EMT	Giamarelos Nikolaos, Mavromatakis Jason, Alifragkis Vagelis

This project has received funding from the European Union's Horizon 2020 research and innovation programme under grant agreement N°864283

Summary

1.1 Summary of Deliverable

This document outlines all the algorithms that are to be developed in the context of the ebalance-plus activity in order to enable the grid Resilience and Reliability. There are five algorithms in total, which are:

1. **Volt/VAr optimization with RES Variability**
2. **Monitor power peaks and voltage violations and request support on lower management units**
3. **Fault Detection, Isolation & Restoration – FDIR**
4. **Simulation of intentional islanding and load shedding to prevent cascading failures**
5. **LV Transformer Status monitoring with PMU and sensors**

Each of the above is analyzed in its own section with the following logic:

1. **Present the state of the art for each algorithm based on bibliographic research**
2. **Present the scope and the applicability of the algorithm in the context of the activity**
3. **Present the technical steps (to be) performed to implement the algorithm.**
4. **Present the steps to be perform in to validate and demonstrate the algorithm.**

Before presenting each algorithm separately, we firstly present an approach for integrating the algorithms with the ebalance-plus middleware and the target hardware devices.

Finally, after the presentation of each algorithm, we briefly outline perceived benefits when used in conjunction with the ebalance-plus Framework.

Disclaimer

This project has received funding from the European Union's Horizon 2020 research and innovation programme under grant agreement N°864283

Table of Contents

This project has received funding from the European Union's Horizon 2020 research and innovation programme under grant agreement N°864283

Table of tables

Table of figures

This project has received funding from the European Union's Horizon 2020 research and innovation programme under grant agreement N°864283

Abbreviations

API	Application Programming Interface
CEP	Complex Event Processor
MAS	Modal Analysis
U_c	Declared supply voltage
U_n	Nominal voltage of the system
P_{st}	Short term flicker severity, measured over a period of ten minutes.
P_{lt}	Long term flicker severity, calculated from a sequence of 12 P_{st} – values over a two-hour interval.
PMU	Phasor Measurement Unit
PV	Photovoltaic
WF	Wind Farm

This project has received funding from the European Union's Horizon 2020 research and innovation programme under grant agreement N°864283

1 Introduction

1.1 Power grid resilience and reliability

A literature review on electric power grid resilience (hence "grid resilience") reveals a not-yet standardized definition and that there are also economic, social and policy aspects beyond the technical one [AD-1]. As the general term of resilience dictates, grid resilience implies the recovery rate from service disruption. According to the Intergovernmental Panel on Climate Change (IPCC), resilience is a system's ability to anticipate, absorb, and recover from the effects of hazardous events in a timely and efficient manner [AD-2]. Essential properties of a resilient system are avoiding service disruption through **anticipation/prevention**, minimizing damages caused by hazardous events (**absorption/degradation**), restarting/rebuilding its functionalities (**recovery/restoration**) and learning from past such events (**adaptation**) in order to deal with future ones. Events considered as hazardous are mainly related to extreme weather causing outages that can leave customers without power in numbers ranging from 100k to several millions (84% of global power grid faults are attributed to natural causes).

The aforementioned resilience properties are visualized for a functioning grid over time (Figure 1.1) as an "Attack" on the grid takes place at time t_E and the transition to the states of degradation and restoration form a "resilience triangle".

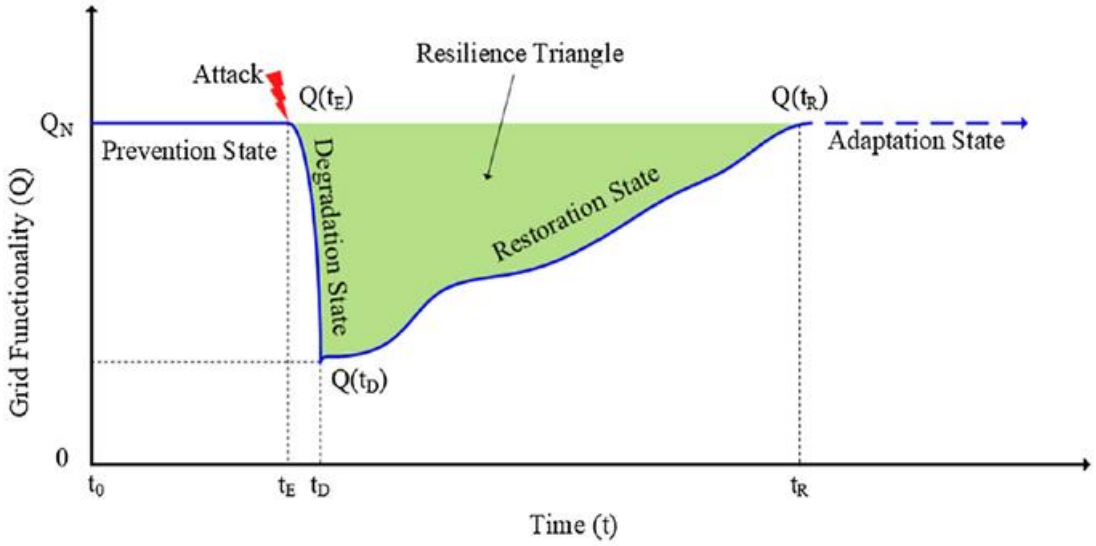

Figure 1.1: Grid resilience states associated with a hazardous event (source: [AD-1])

An important element of the grid resilience aspect is its infrastructure which is considered critical as it enables core societal, economic and technological functions. Infrastructure level malfunctions can either happen at transmission or distribution level with the later presenting the highest possibility of causing customer service disruption (see Table 1-1).

This project has received funding from the European Union's Horizon 2020 research and innovation programme under grant agreement N°864283

Table 1-1 Infrastructure levels of malfunctions and their likelihood of causing disruptions (source: Copenhagen Economics illustration)

Infrastructure level	Examples for causes for malfunctions	Likelihood of disruption in case of malfunction	Intuition
Distribution	Tree falling on a distribution (overhead) line, malfunction of a transformer station, storms damaging the (overhead) lines	high, but smaller area	Distribution lines and cables are often the sole source of supply to a (small) area
Transmission	Outage in an interconnector in the transmission grid, snow or storms damaging overhead transmission lines	low to high, larger area	Typically, a transmission line or cable – especially an interconnector – is not the only source of supply to an area. In case of a malfunction, electricity is supplied through other transmission cables or lines

A notion related to grid resilience is **grid reliability**: IEEE defines it as the grid's required performance for given conditions and time interval [AD-3]. Within this context, grid reliability is examined for the frequency and duration of system interruption caused by common failures like short circuits or malfunctioning devices. An overview of the differences in aspects of grid resilience and reliability can be observed in Table 1-2 and a conclusion drawn is that a reliable grid is not necessarily evaluated as resilient.

Table 1-2 Differences in aspects of grid resilience and reliability (author's table based on [AD-4])

Grid notion	Hazardous event probability	Hazardous event impact	System focus	Concern
Resilience	Low	High	Transition time between states	Infrastructure recovery time
Reliability	High	Low	State	Customer interruption time

In [AD-5], the authors - after their literature review - clustered the solutions to grid faults in four main clusters:

1. **Prevention and management (28%): mainly physical hardening of the infrastructure (underground lines, elevating substations, preventive maintenance).**
2. **Monitoring and fault detection (20%): mainly real-time monitoring through SCADA systems for faults and load imbalances.**
3. **Smart grid-based solutions (33%): mainly interconnected microgrids and intentional islanding.**

This project has received funding from the European Union's Horizon 2020 research and innovation programme under grant agreement N°864283

4. **Modeling and simulation (23%): mainly extreme weather modelling and simulation of cascading failures.**

Smart-grid based solutions take the largest share for grid resilience because in smart-grids problems are detected and operators are alerted in near real-time, while the topology can be reconfigured to offer alternative routes for power delivery. With DER, energy generation and consumption take place locally or very near to demand and the impact of damaged grid components (at infrastructure level like transmission and distribution lines) by extreme events is reduced. Microgrids through islanding can operate independently from the main grid thus becoming a major driver for implementation especially in geographical areas with extreme weather events (e.g. USA). Studies are conducted for microgrid size, location and operation under different objective functions (investment cost, level of resilience, etc.). Proactivity can be provided by means of smart-grid simulation and estimation of current and future states under various scenarios of resilience and reliability aspects.

1.2 The ebalance-plus ecosystem

The solutions to be developed within the ebalance-plus project are built around the major component of the project – the ebalance-plus energy management platform. The hierarchical approach followed in the project allows to involve different smart-grid innovations (smart production, storage and consumption technologies, etc.) and to realize distributed and scalable energy control. The approach exploits the actual topology of the energy grid and makes use of computational elements (management units - MUs) that are located on the joints of the grid topology branches, to be closer to the monitored and controlled assets, enabling the decision-making process to be local. These MUs are located on different levels of the grid and manage all the lower-level management units, but also additional elements, like sensors and actuators, located in their branch (see Figure 1.2). Similar to a fractal, depending on the level of the considered MU, the monitored parameters and control tasks are the same, but they differ in the scale. This allows developing generic algorithms that can be deployed on the MUs in the smart grid in order to realize many different tasks. This allows monitoring resilience-related parameters on different levels of the grid and applying local and appropriate actions to cope with the disturbing events.

This project has received funding from the European Union's Horizon 2020 research and innovation programme under grant agreement N°864283

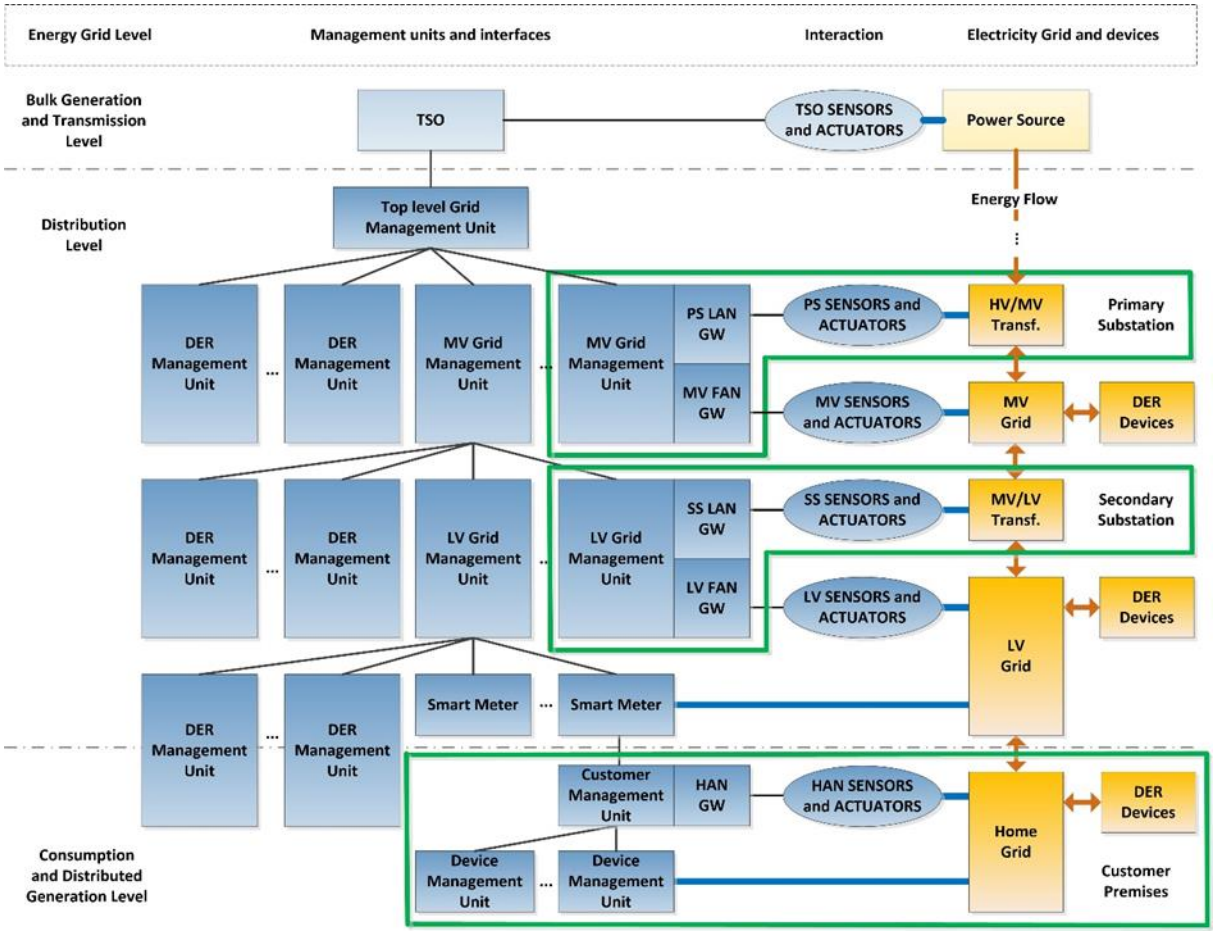

Figure 1.2 The naming and distribution of management units within the energy grid

1.3 The ebalance-plus energy balancing platform

The management units are parts of the distributed energy management platform. These exchange the data being the measurements as well as the control signals to monitor and control the grid assets. The data exchange is realized based on the middleware and the energy management components (like the algorithms) reside on top of it. Each management unit expresses the similar architecture of the energy management platform, but the exact set of algorithms and other components may differ depending on the specific deployment. The generic architecture of the Energy Management Platform is shown in Figure 1.3 - within the presented management unit the EMP consists of four components: the GUI to interact with the user, the EMP Coordinator that manages all the other EMP components, and two components that perform the energy management related to energy flexibility and resilience. All these components exchange data using the middleware. They all also interact with the grid assets (via measurements and control signals) using adapters (that are not reflected in this figure).

This project has received funding from the European Union's Horizon 2020 research and innovation programme under grant agreement N°864283

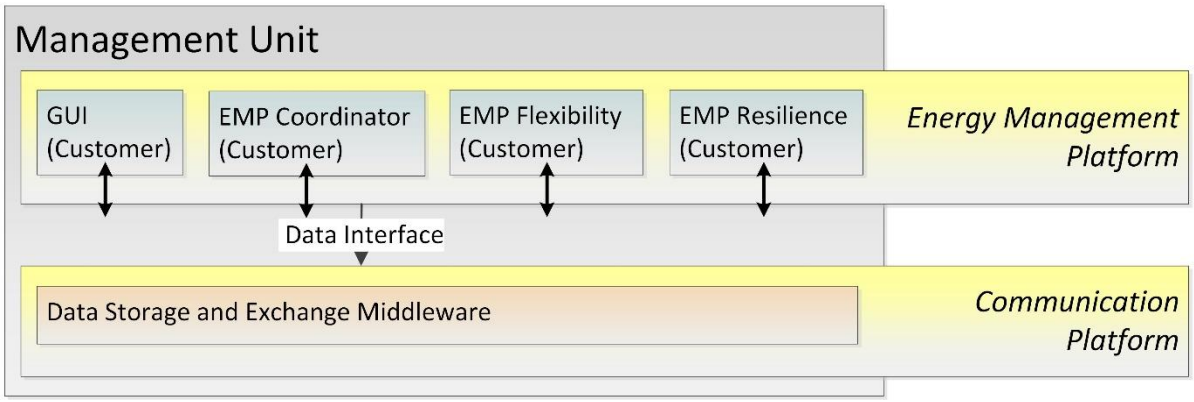

Figure 1.3 The generic architecture of the ebalance-plus Energy Management Platform

The details on the Energy Management Platform are provided in ebalance-plus deliverable D4.3.

2 Current Infrastructure

2.1 High Level Design

The current activity is comprised by the two major constituents. Firstly, the algorithms themselves for each use case need to be defined in terms of operation and logic. Secondly, the interaction with the rest of the system via the ebalance-plus platform needs to also be taken into account so as to assure the best possible integration with the rest of the system. To meet these goals, instead of providing each algorithm as a single monolithic component, a framework that generalises common aspects across the different algorithm implementations has been defined.

More specifically, the following needs have been identified across use cases and algorithms:

1. Interaction with ebalance-plus Framework for Input / Output operations
2. KPI calculation and propagation for each algorithm
3. Synchronous / Asynchronous operation of the underlying algorithm
4. Configuration facility for the underlying algorithm.

The above can be considered as separate components that interact to provide the target operation. The following are depicted at a high-level in Figure 2.1. The dark blue colour defines reusable entities, the light blue colour defines entities that need specialization per algorithm and the grey colour defines external elements.

This project has received funding from the European Union's Horizon 2020 research and innovation programme under grant agreement N°864283

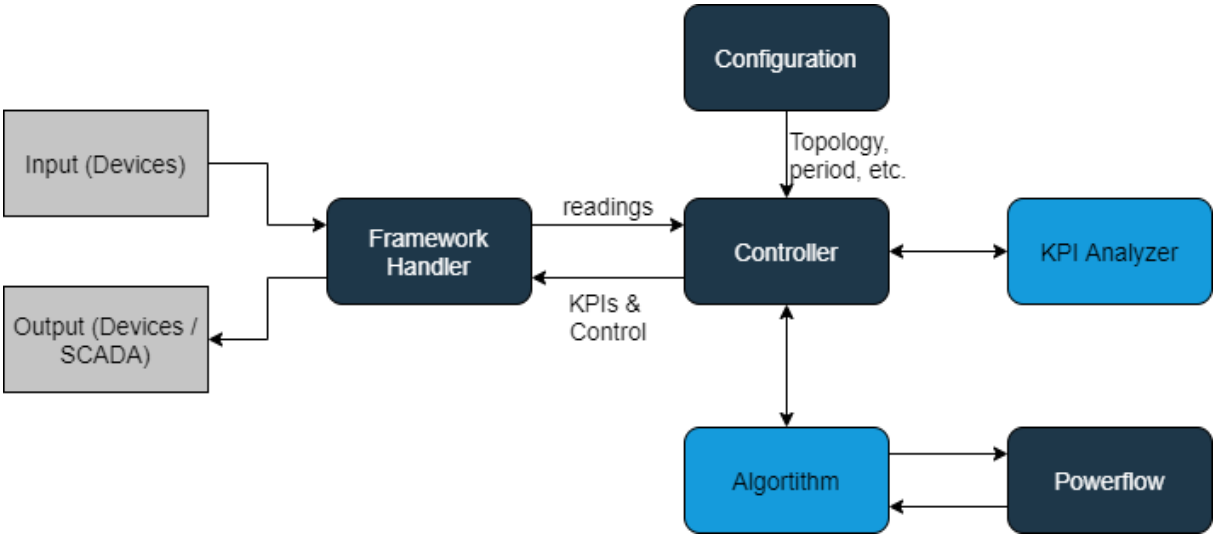

Figure 2.1 High Level Framework Infrastructure

The controller forms the main component of the framework and it synchronizes every other component. Specifically, it performs the following actions:

1. Instantiate all other components and interconnect them
2. Synchronize execution of the framework

The framework handler is responsible for interacting with the ebalance-plus Framework in order to receive the necessary inputs and provide the necessary outputs. While the exact inputs and outputs are dependent on the algorithm, the manner of interaction with the ebalance-plus framework is not. As such, the Framework Handler is a highly configurable component that completely abstracts the communication layer from the rest of the application.

The configuration component is responsible for handling all the configuration needs both for the algorithm itself and for the rest of the framework. Initially, it acts as file parser for any kind of file the application needs. The application relies on JSON files for its configuration. All other components have access to the Configuration components in order to retrieve the values they need.

The power-flow component is a wrapper for the python PandaPower library. PandaPower is extensively used for power system modelling, analysis and optimization [AD-95], [AD-96], [AD-97], [AD-98] as it presents a lot of advantageous features. PandaPower is implemented in Python, guaranteeing free availability and flexible expansion with other open-source libraries. Since it is developed as a cross-platform library, it can be deployed seamlessly on computational clusters and parallelized without any license constraints. All implementations are thoroughly verified and wherever possible validated by comparing with commercial software tools. PandaPower has been successfully applied in multiple grid studies [17], [18], [19], [20]. Because of the comprehensive model library and the easy-to-use Python interface, PandaPower has a relatively low entry barrier for new users to perform basic power systems analysis. It forms the main constituent for power-flow and optimal power flow solving. Its main configuration is the topology of a specific grid which is inputted to the library as a YAML file.

This project has received funding from the European Union's Horizon 2020 research and innovation programme under grant agreement N°864283

The last two components are the Algorithm and the KPI Analyser. Both of those are specific to each algorithm in terms of implementation. However, they offer a specific interface for the rest of the framework to access them. While the inputs and outputs of those are specific for each algorithm there are some common elements such the topology being used and the optimization objective.

2.2 Deployment

The complete framework will be deployed on appropriate management unit (MU) depending on the needs of the underlying algorithm. The available management units are the DERMU, the LVGMU and the MVGMU (D3.4 - Specification and implementation of grid automation and control devices and interfaces). Each of these devices supports a Linux operating system upon which Python will be executed. All communication with external entities will be based on the ebalance-plus Platform. The main deployment approach is depicted in Figure 2.2.

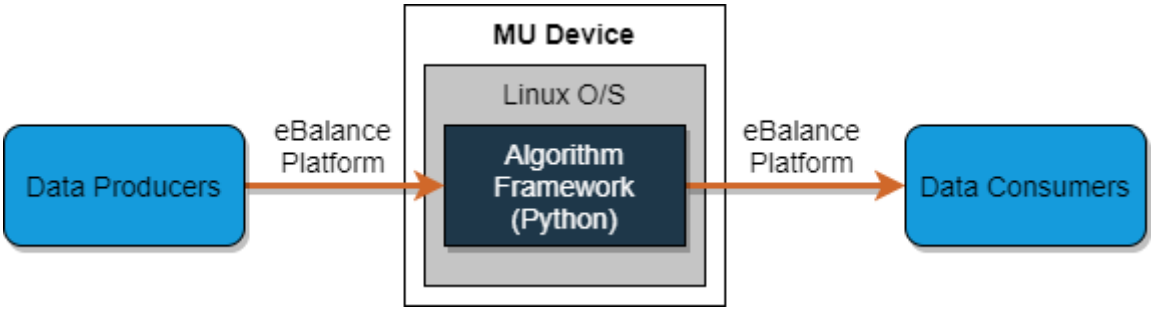

Figure 2.2 Main Algorithm Framework Deployment

Before the actual deployment on the devices however, an intermediate step is needed where all deployment occurs locally in order to accommodate algorithm validation. In this setup the MU device is replaced by a Linux Host Computer where the algorithms can run in the same way as they were deployed on the MU device. Additionally, Data Producers are replaced by appropriate simulators in order to perform the algorithm excitation with reasonable inputs. To accommodate all of the above, an ebalance-plus platform server is also deployed on-premises to act as the intermediary and enable the use of the ebalance-plus platform. The concept is depicted in Figure 2.3.

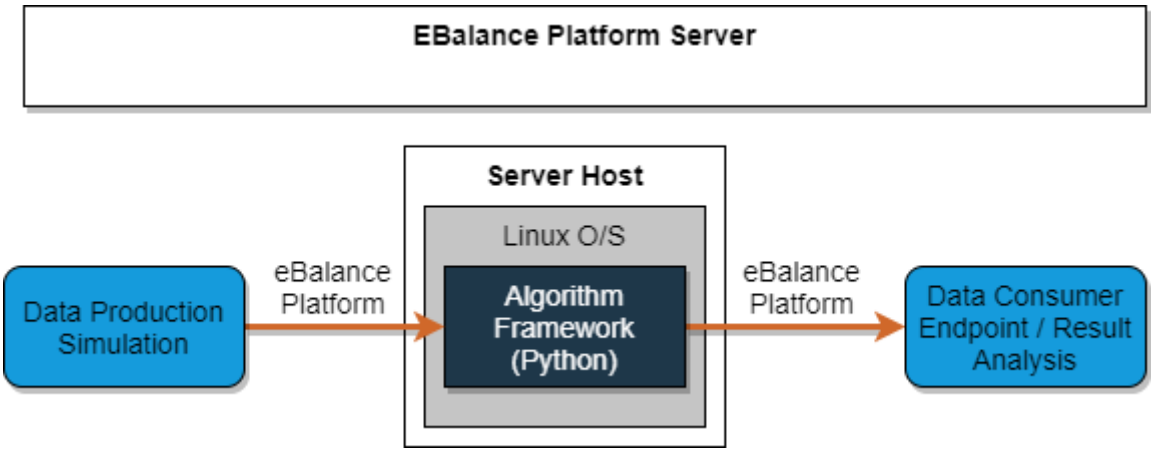

Figure 2.3 Algorithm Framework Deployment for validation

This project has received funding from the European Union's Horizon 2020 research and innovation programme under grant agreement N°864283

More detail about the MUs is provided in the D3.4 - Specification and implementation of grid automation and control devices and interfaces. Essentially, the MUs are the low-level components that enable the actuation between the algorithms and the corresponding equipment, sensors, actuators, and devices that need to be controlled and read data from using the appropriate interfaces that are commonly used in power grid management applications. In summary, the three MUs are briefly presented below:
MVGMU: Medium Voltage Grid Management Unit, this device is installed in medium to low voltage distribution substations and its main function is to monitor the substation transformer, measure the grid voltage and current, and to automate the reactive power compensation in power distribution substations.
LVGMU: Low Voltage Grid Management Unit, this device is installed near the low-voltage transformer and its function is to continuously measure the voltage and the current of the grid to provide a set measurement to the higher level where decisions are taken based on adjustable criteria. Additionally, the LVGMU supports the synchronization of measurements between different MUs using GPS to provide the ability for further analysis and to easily correlate the occurrences of specific chain of events.
DERMU: Distributed Energy Resources Management Unit, this is a compact device that supports edge computing, like all other MUs, and it's installed in photovoltaic parks, wind farms etc. where the management of energy resources is crucial for the operation of the grid. The device includes a set of commonly used interfaces to support a wide selection of external devices and equipment to be connected (Diesel generators, Inverters etc.)

This project has received funding from the European Union's Horizon 2020 research and innovation programme under grant agreement N°864283

3 Volt/VAr optimisation with RES variability

3.1 State of the art

Volt/VAr control in the distribution network takes place in real time and aims at balancing reactive power, with simultaneous control of voltage and frequency in the network, within specific limits. Voltage control is imperative, as it is necessary to protect the network equipment and the consumer from overvoltages and undervoltages. It is primarily achieved by means of load tap changers (LTC) on the transformers of substations. LTCs usually act automatically and control the voltage in the secondary winding of the transformer. The main objective of Volt/VAr control methods is to compensate for inductive loads (without overshoots that can lead to high losses), while indirect control of the voltage in the distribution network is carried out secondarily.

Unfortunately, the increased penetration of RES makes it difficult to keep the voltage within acceptable limits. Traditional control methods, with individual actions on the substations, often suffer from inelasticity and therefore fail to control the system. For example, there is a physical limitation on the control movements that an LTC can make in a given time period. In addition, it is often not economically feasible for the LTC to reinforce these devices (or the grid itself) to deal with surges. Thus, combined and coordinated control actions are required to manage the problem with existing equipment [AD-6].

RES may initially introduce additional difficulties in managing support functions, but, with proper control, they can eventually be used to enhance the latter [AD-24]. In particular, RES inverters have the potential to provide support functions to the distribution network, involving reactive power compensation, voltage and frequency control [AD-25], [AD-26]. To achieve this scheme, however, a decentralized method of controlling the RES generation is required.

Automatic Volt/VAr distribution network control has traditionally followed centralized control strategies involving LTC and capacitor array control. These controllers were traditionally based on simple rules, but there are approaches based on more sophisticated techniques, such as the MPC methodology [AD-6]. Nowadays, the current research interest is mainly focused on distributed control using shifting loads, or reactive load injections from RES inverters. The simplest implementation is local, or autonomous control [AD-7] in which the agents have no communication, which means that the control scheme does not exploit the full potential of the system and can also lead to instability in cases of non-continuous operation.

Control with distributed optimization reduces to decomposing the OPF problem and solving it by distributed algorithms. Distributed optimization algorithms such as ADMM and DD can guarantee convergence to the total optimum for convex OPF problems [AD-8], but require a centralized per-step computation to solve the dual step [AD-9] (there are of course solutions that overcome this difficulty, as in reference [AD-10]). Distributed gradient-based methods for Volt/VAr control with a focus on robustness of

This project has received funding from the European Union's Horizon 2020 research and innovation programme under grant agreement N°864283

control take place in references [AD-11] and [AD-12], where approaches capable of handling communication failures between agents, or inaccuracies in the modelling of the OPF problem are presented. Some drawbacks of these methods are that the convergence rate is affected by the quality of communication, in particular the "ping" between agents. Also, asynchronous communication between agents is a real issue in a real implementation, so it must be taken into account.

There is high research interest in the issue of consensus algorithms for control via distributed Volt/VAr cooperation [AD-13], [AD-14]. "Consensus" is influenced by the consensus protocol and greatly affects the performance of the control scheme, with the weighted-average consensus algorithm enjoying the most widespread implementation [AD-15]. The stability of the algorithms can be demonstrated for small set-point changes, but the communication drawbacks mentioned in the previous paragraph apply here as well. The distributed MPC approach is also interesting, which is relatively modern in Volt/VAr control [AD-16] and can handle cases of parameter uncertainty during modelling, with the disadvantage of increased computational load.

An intermediate Volt/VAr control scheme is zone-based control, where the distribution network is fragmented into control regions where some distributed method is applied. The regions can be "coupled" through a common node so that the entire network converges to a particular state [AD-17]. The overall scheme may even be hierarchical and incorporate traditional control movements for voltage control, combining ADMM method for short-term control of RES and some classical technique for solving the MINLP problem of long-term control of LTCs and capacitor arrays [AD-18].

In general, zone-based control methods are characterized by ease of integration (plug-n-play ability) as they can comply with the existing operating regime: the central distribution grid operator retains its role, while the RES generators will be grouped (aggregation) into control zones based on ownership, or other criterion. Thus, the former will be able to issue grid control instructions, and the latter will be able to execute them, with minimal knowledge of system details on both sides. Such an approach has been piloted on the Greek island of Kythnos [AD-19]. Finally, a disadvantage of these methods is that control failure due to loss of communication can affect an entire region, unlike a fully distributed approach [AD-20].

3.2 Scope

As already stated, Volt/VAr control aims primarily to minimize voltage drop (VD) and rise violations (eq. 1). During this task, the control variables (tap movement rate of transformers, curtailed power of PV and reactive power of PV inverter) are optimized and then the control actions applied within an iterative loop. For the purposes of this study, the minimization of power losses (eq. 2) and RES curtailment (eq. 3) are defined as further objectives.

$$VD = \sum_{i=1}^{N} |V_i - V_i^{sp}| \quad (1)$$

where V_i^{sp} is the pre-specified reference voltage value at i-th load bus, which is usually set at the value of 1.0 per unit (p.u.) and N is the number of load buses.

$$P_{LOSS} = \sum_{i=1}^{m} R_m |I_m|^2 \quad (2)$$

This project has received funding from the European Union's Horizon 2020 research and innovation programme under grant agreement N°864283

where P_{LOSS} is the total active power losses in the distribution network, m is the branch number, R_m is the resistance in the branch m and I_m is the current in the branch m.

$$CP = \sum_{m=1}^{M} CFPV_m \times \left(PPV_{max,m} - PPV_m\right) + \sum_{n=1}^{N} CFWF_n \times \left(PWF_{max,m} - PWF_m\right) \quad (3)$$

where $CFPV_m$ is a weight factor of the curtailed power of the m-th PV unit, with $\sum_{m=1}^{M} CFPV_m = 1$, $PPV_{max,m}$ and PPV_m represent, respectively, the maximum and actual power of the m-th PV unit, $CFWF_n$ is a weight factor of the curtailed power of the n-th WF unit, with $\sum_{n=1}^{N} CFWF_n = 1$, $PWF_{max,m}$ and PWF_m represent, respectively, the maximum and actual power of the n-th WF unit.

The underlying constraints of the Volt/VAr optimization problem are listed below:

- Node voltage limits, i.e. upper and lower limits of the acceptable voltage fluctuation (1 being nominal)
- Transformer constraints, (e.g. TAP max and min positions. All constraints are demonstrated in figure **Figure 3.4**)
- Line loading limits, expressed as a percentage of the acceptable current load on a line
- External grid active and reactive power injection limits, which demonstrate the maximum and minimum MW and MVAr that can be injected by the external grid (i.e. the slack bus)
- Upper and lower limits of the curtailed power of each RES unit, i.e. a range that defines how much power will be used from the total production of a RES unit
- Upper and lower limits of the reactive power of PV inverters, which defines the acceptable range of the set-point.

3.3 Technical Methodology

3.3.1 Operation Overview

The Volt/VAr algorithm requires two elements to operate correctly. Firstly, a configuration is needed to define mainly the grid topology and the algorithm's target objective. The configuration is only needed once during the initialization phase. Secondly, the algorithm requires a set of inputs that define the real time state of the grid at each execution. These inputs are gathered from the underlying elements of the grid and concern load consumptions, RES generation, capacitor and TAP states. After the execution of the algorithm, two kinds of outputs are produced. The first concerns commanding and controlling the underlying elements of the power grid and specifically, for the Primary Substation (P/S), the Secondary Substation (S/S) and the RES elements. The second concerns a series of KPIs that define the performance of the algorithm. The high-level architecture of the algorithm in terms of inputs and outputs is depicted in Figure 3.1.

This project has received funding from the European Union's Horizon 2020 research and innovation programme under grant agreement N°864283

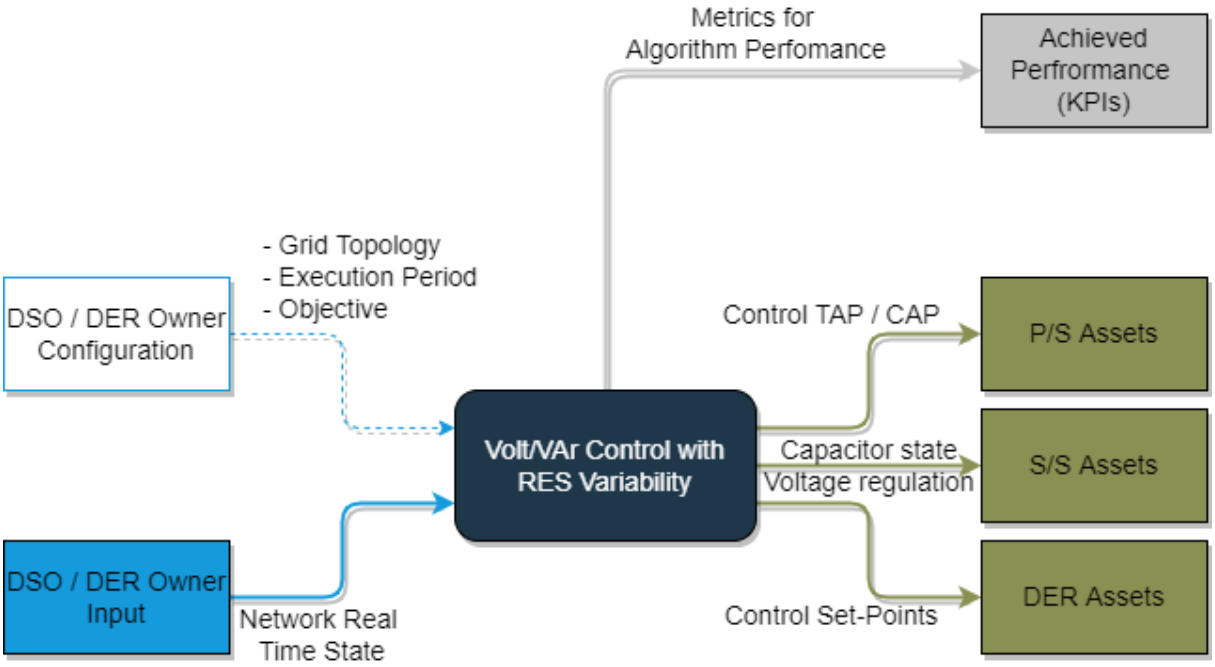

Figure 3.1 High-level block-diagram for Volt/VAr Algorithm

As the algorithm is executed periodically, several steps are taken in order to compute the target output as shown in Figure 3.2.

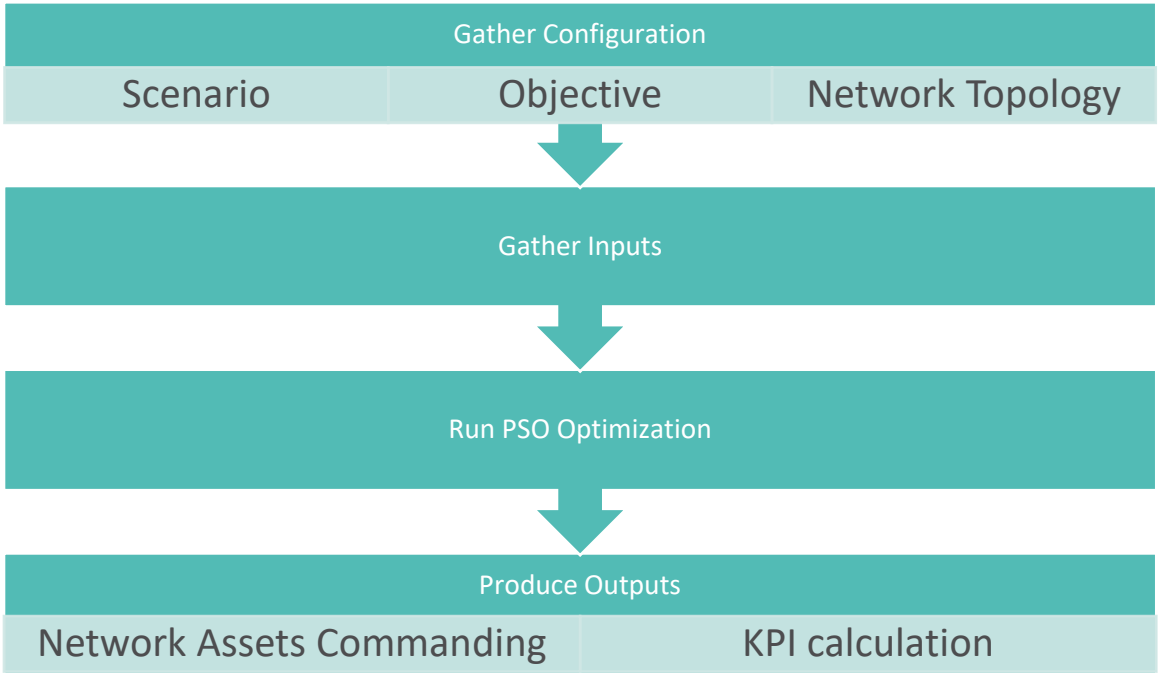

Figure 3.2 Volt/VAr execution process

The first step concerns the retrieval of the algorithm's configuration from the appropriate component. The configuration are: Network Topology, Target Scenario, and Target Objective.

The Network Topology is comprised by the following elements:

1. **Lines (length, conductance, bus connections)**

This project has received funding from the European Union's Horizon 2020 research and innovation programme under grant agreement N°864283

2. **Buses (grid voltage level, min/max bus voltage)**
3. **Switches (state, bus connections)**
4. **Loads (location, active and reactive power, min/max active and reactive power)**
5. **Diesel Generators (rated power)**
6. **RES Generators (location, nominal power, active and reactive power, min/max active and reactive power)**
7. **Transformers (high voltage bus, low voltage bus, rated apparent power, rated voltage on high voltage, rated voltage on low voltage, real part of relative short-circuit voltage, maximum current loading, relative short-circuit voltage, losses, phase shift angle, min/max tap position, rated tap position)**
8. **Capacitors (location, shunt active power, shunt susceptance, rated voltage, step of shunt)**
9. **Controllable Elements (i.e., any of the above that should be controlled by the algorithm, for a specific example see Figure 3.5)**

The Target Scenario can be either centralized or distributed Volt/VAr optimization with RES Variability while the objectives available are

1. **Voltage Violations Minimization**
2. **RES Curtailment Minimization**
3. **Power Losses Minimization**

Having gathered the needed configuration, the algorithm requires its input which is the current state of the grid. The elements that define the state are:

1. **Voltage at slack bus of distribution grid**
2. **Active power of RES and loads**
3. **Reactive power of RES and loads**
4. **Transformers' TAP position**
5. **Capacitors' bank status**
6. **Line capacitors' status**

Finally, the PSO (Particle Swarm Optimization) Algorithm (discussed in more detail in section 2.3.2) is executed and the outputs are produced as follows:

a. **Network Assets Commanding**
    a. **Capacitors' bank new status**
    b. **Transformers' TAP position**
    c. **Line capacitors' status**
    d. **RES set-points**
b. **KPI Calculation**
    a. **Voltage violations frequency**
    b. **Voltage violations count**
    c. **Voltage violation duration**
    d. **Voltage violations excess**
    e. **Power losses**
    f. **RES energy**
    g. **RES curtailment percentage**
    h. **Number of capacitor switches**
    i. **Number of OLTC switches**

This project has received funding from the European Union's Horizon 2020 research and innovation programme under grant agreement N°864283

3.3.2 Optimization process

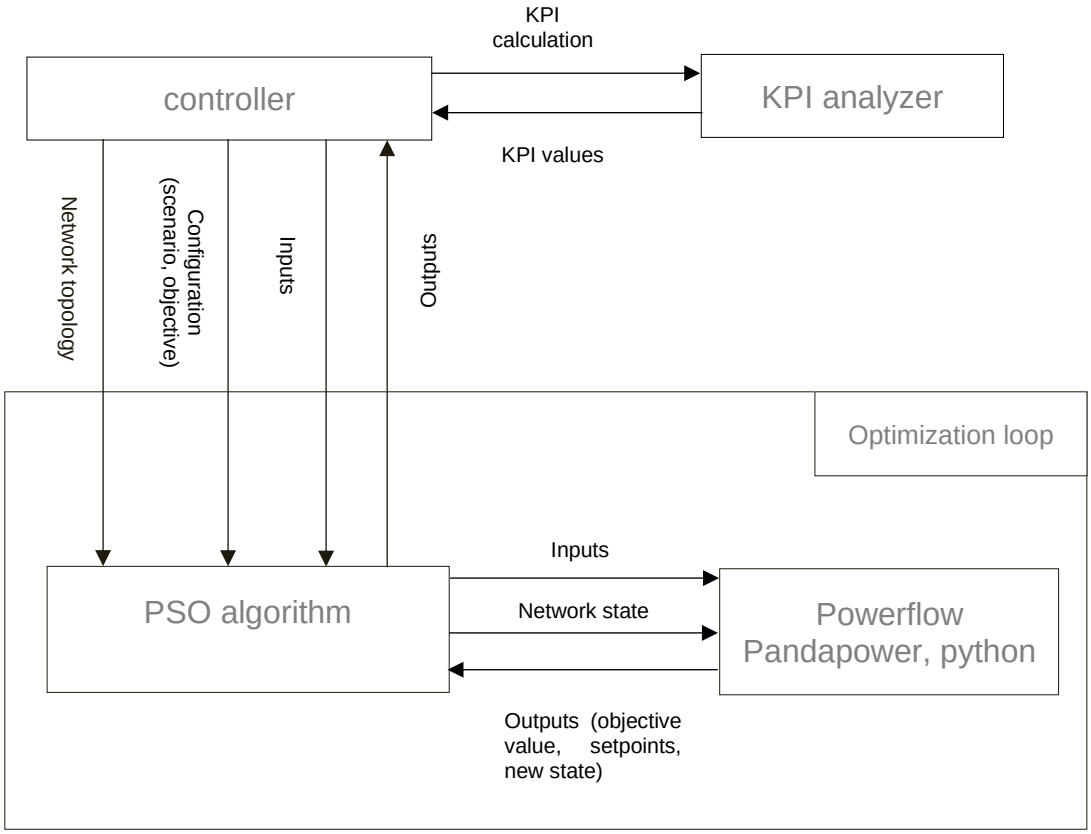

Figure 3.3 Optimization backend

The purpose of this program is to wrap pandapower functionalities and place them in a more general context that extends the above capabilities through interfacing with other programming languages such as MATLAB. The functionalities regard:

1. Network element creation
2. Network diagnostics
3. Network plotting and result visualization
4. Power flow algorithms
5. Network optimization

This extension allows for the application of optimization and control modules not normally present in pandapower (or Python).

1. The program attempts to follow the 'logic' of pandapower as closely as possible, namely by consolidating all network creation, KPI & state calculation and variable mapping operations in one object (net_handle.py). This object is then passed around to the other modules for the application of optimization (net_optimization.py) and result handling (postprocessing_utilities.py) operations.
2. The program can apply optimal power flow operations for a network snapshot, as well as control operations for a network timeseries. NOTE: The control

This project has received funding from the European Union's Horizon 2020 research and innovation programme under grant agreement N°864283

operations on timeseries is static, i.e. it is just sequential evaluations of network snapshots, which is identical to what the pandapower timeseries module does.

The program accepts as inputs:

1. **A YAML file describing the network architecture.** An example of the form of this file is given in Figure 2-4 for a random architecture. Here, all elements of the grid are specified, including those that can be controlled in the case of optimization (controllable elements).
2. **A .csv file containing the values of all time variant elements of the grid,** such as loads and photovoltaic generations. This .csv is called a snapshot if it describes a single network time instant (snapshot), or timeseries if it describes multiple time instants (timeseries). An example snapshot that corresponds to the architecture file of Figure 2-4 is given in Figure 2-5.
3. **A YAML file describing the configuration of the optimization.** An example is provided in Figure 2-6 for the case of real power losses minimization.

This project has received funding from the European Union's Horizon 2020 research and innovation programme under grant agreement N°864283

```
Architecture:
  Bus:                          ### The buses of the network are defined here.
                                ### Following the explanation of each bus key
                                ### is given
    - name: "BUS_0"             ### name of this bus
      vn_kv: 150                ### the grid voltage level
      type: 'b'                 ### type of this bus
      max_vm_pu: 1.05           ### maximum bus voltage in p.u..
      min_vm_pu: 0.95           ### minimum bus voltage in p.u
    - name: "BUS_1"
      vn_kv: 20
      type: 'b'
      max_vm_pu: 1.05
      min_vm_pu: 0.95
    - name: "BUS_2"
      vn_kv: 20
      type: 'b'
      max_vm_pu: 1.05
      min_vm_pu: 0.95
    - name: "BUS_3"
      vn_kv: 20
      type: 'b'
      max_vm_pu: 1.05
      min_vm_pu: 0.95
    - name: "BUS_4"
      vn_kv: 20
      type: 'b'
      max_vm_pu: 1.05
      min_vm_pu: 0.95
    - name: "BUS_5"
      vn_kv: 0.23
      type: 'b'
      max_vm_pu: 1.05
      min_vm_pu: 0.95
   - name: "BUS_6"
     vn_kv: 0.23
     type: 'b'
     max_vm_pu: 1.05
     min_vm_pu: 0.95
```

This project has received funding from the European Union's Horizon 2020 research and innovation programme under grant agreement N°864283

```
Line:                       ### The lines of the network are defined here.
                            ### Following the explanation of each line key is
                            ### given
  - name: "LINE_1"          ### name for this line
    from: 'BUS_1'           ### ID of the bus on one side which the line will
                            ### be connected with
    to: 'BUS_2'             ### ID of the bus on the other side which the line
                            ### will be connected with
    length_km: 3            ### The line length in km
    c_nf_per_km: 0          ### line capacitance in nano Farad per km
    g_us_per_km: 0.0        ### dielectric conductance in micro Siemens per km
    df: 1.0                 ### derating factor: maximal current of line
                            ### in relation to nominal current of line
                            ### (from 0 to 1)
    in_service: true        ### True for in_service or False for out of
                            ### service
    max_i_ka: 4             ### maximum thermal current in kilo Ampere
    parallel: 0             ### number of parallel line systems
    r_ohm_per_km: 0.0011    ### line resistance in ohm per km
    x_ohm_per_km: 0.0011    ### line reactance in ohm per km
    type: ol                ### type of line (“ol” for overhead line
                            ### or “cs” for cable system)
    max_loading_percent: 90 ### maximum current loading
  - name: "LINE_2"
    from: 'BUS_2'
    to: 'BUS_3'
    length_km: 1.5
    c_nf_per_km: 0
    g_us_per_km: 0.0
    df : 1.0
    in_service: true
    max_i_ka: 4
    parallel: 0
    r_ohm_per_km: 0.0015
    x_ohm_per_km: 0.0032
    type: ol
    max_loading_percent: 90
  - name: "LINE_3"
    from: 'BUS_3'
    to: 'BUS_3'
    length_km: 1
    c_nf_per_km: 0
    g_us_per_km: 0.0
    df: 1.0
    in_service: true
    max_i_ka: 4
    parallel: 0
    r_ohm_per_km: 0.0015
    x_ohm_per_km: 0.0032
    type: ol
    max_loading_percent: 90
  - name: "LINE_4"
    from: 'BUS_5'
    to: 'BUS_6'
    length_km: 1
    c_nf_per_km: 0
    g_us_per_km: 0.0
    df: 1.0
    in_service: true
```

This project has received funding from the European Union’s Horizon 2020 research and innovation programme under grant agreement N°864283

```
Switch:              ### The switches of the network are defined here.
                     ### Following the explanation of each switch key
                     ### is given
  - name: 'SW_1'     ### The name for this switch
    from: 'BUS_2'    ### ID of the bus on one side which the switch will
                     ### be connected with
    to: 'BUS_3'      ### ID of the bus on the other side which the line
                     ### will be connected with
    et: 'b'          ### element type: “l” = switch between bus and line,
                     ### “t” = switch between bus and transformer,
                     ### “b” = switch between two buses
    type: 'CB'       ### indicates the type of switch: “LS” = Load Switch,
                     ### “CB” = Circuit Breaker, “LBS” = Load Break Switch or
                     ### “DS” = Disconnecting Switch
    closed: True     ### switch position: False = open, True = closed
  - name: 'SW_2'
    from: 'BUS_3'
    to: 'BUS_4'
    et: 't'
    type: 'CB'
    closed: True

Load:                ### The loads of the network are defined here.
                     ### Following the explanation of each load key
                     ### is given
  - name: 'LOAD_1'   ### The name for this load
    bus: 'BUS_6'     ### The bus id to which the load is connected
    p_mw: 0.45       ### The real power of the load
                     ### positive value -> load
                     ### negative value -> generation
    q_mvar: 0.045    ### The reactive power of the load
    scaling: 1       ### An OPTIONAL scaling factor to be set customly
  - name: 'LOAD_2'
    bus: 'BUS_6'
    p_mw: 0.45
    q_mvar: 0.045
    scaling: 1

Static_Generator:    ### The sgens of the network are defined here.
                     ### Following the explanation of each sgen key
                     ### is given
  - name: 'SGEN_1'   ### The name for this sgen
    bus: 'BUS_6'     ### The bus id to which the static generator is connected
    sn_mva: 2        ### Nominal power of the sgen
    p_mw: 0.5        ### The real power of the static generator (negative
                     ### for generation!)
    q_mvar: 0.1      ### The reactive power of the sgen
    scaling: 1       ### An OPTIONAL scaling factor to be set customly
    type: 'PV'       ### type variable to classify the static generator
    max_p_mw: 1      ### Maximum active power injection
    min_p_mw: 0      ### Minimum active power injection
    max_q_mvar: 2    ### Maximum reactive power injection
    min_q_mvar: -2   ### Minimum reactive power injection

External_Grid:     ### The external grid of the network is defined here.
                   ### Following the explanation of each external grid key
                   ### is given
  - name: 'EXT'    ### name of of the external grid
    bus: 'BUS_0'   ### bus where the slack is connected
    vm_pu: 1.05    ### voltage at the slack node in per unit
```

This project has received funding from the European Union’s Horizon 2020 research and innovation programme under grant agreement N°864283

```
    va_degree: 50   ### voltage angle at the slack node in degrees*
    max_p_mw: 10    ### Maximum active power injection.
    min_p_mw: -10   ### Minimum active power injection.
    max_q_mvar: 10  ### Maximum reactive power injection.
    min_q_mvar: -10 ### Minimum reactive power injection.


Transformer:                ### The external grid of the network is
                            ### defined here.
                            ### Following the explanation of each external
                            ### grid key is given
  - name: 'TRAFO_1'         ### A custom name for this transformer
    hv_bus: 'BUS_0'         ### The bus on the high-voltage side on which
                             ### the transformer will be connected to
    lv_bus: 'BUS_1'         ### The bus on the low-voltage side on which
                             ### the transformer will be connected to
    vn_hv_kv: 150           ### rated voltage on high voltage side
    vn_lv_kv: 20            ### rated voltage on low voltage side
    sn_mva: 50              ### rated apparent power
    vkr_percent: 0.41       ### real part of relative short-circuit voltage
    max_loading_percent: 60 ### acceptable maximum current loading
    vk_percent: 18          ### relative short-circuit voltage
    pfe_kw: 22              ### iron losses in kW
    i0_percent: 0.04        ### open loop losses in percent of rated current
    shift_degree: 50        ### Angle shift over the transformer*
    tap_max: 10             ### maximal allowed tap position
    tap_min: 0              ### minimal allowed tap position
    tap_neutral: 5          ### tap position where the transformer ratio
                            ### is equal to the ration of the rated voltages
    tap_side: 'hv'          ### position of tap changer ("hv", "lv")
    tap_pos: 0              ### current tap position of the transformer
    tap_step_percent: 1.5   ### tap step size for voltage magnitude in
                           ### percent
    tap_step_degree: 0      ### tap step size for voltage angle in degree*
    tap_phase_shifter: False ### whether the transformer is an ideal phase
                            ### shifter*
  - name: 'TRAFO_2'
    hv_bus: 'BUS_4'
    lv_bus: 'BUS_5'
    sn_mva: 0.4
    vn_hv_kv: 20
    vn_lv_kv: 0.23
    vkr_percent: 1.425
    max_loading_percent: 60
    vk_percent: 6
    pfe_kw: 1.35
    i0_percent: 0.3375
    shift_degree: 10
    tap_max: 10
    tap_min: 0
    tap_neutral: 5
    tap_side: 'hv'
    tap_pos: 0
    tap_step_percent: 1.5
    tap_step_degree: 0
```

This project has received funding from the European Union's Horizon 2020 research and innovation programme under grant agreement N°864283

```
LOAD_1/p_mw,LOAD_1/q_mvar,LOAD_2/p_mw,LOAD_2/q_mvar,SGEN_1/p_mw,datetime
0.45,0.045,0.45,0.045,0.5,8/28/2020 10:00
```

Figure 3.4 Snapshot example for a random network

```
Controllable_Elements:      ### The design variables are defined here
  SGEN_1:
    phi:                    ### declare phase angle as design variable
                            ### The phase angle is given by the angle
                            ### between the active power vector, and apparent
                            ### power vector
      type: 'continuous'    ### type of design variable ('continuous' or 'discrete')
      upper: 30             ### upper limit of phase angle phi
      lower: -30            ### lower limit of phase angle phi
    ap_curtailment:         ### declare the curtailment percentage of the active power
                            ### injected by the PV inverter as design variable
      type: 'continuous'    ### type of the design variable
      upper: 0.8            ### upper limit of the ap curtailment percentage
      lower: 0              ### lower limit of the ap curtailment percentage
```

Figure 3.5 Controllable element example

This project has received funding from the European Union's Horizon 2020 research and innovation programme under grant agreement N°864283

```
kpi_config:                    ### Define the objective configuration
  which_kpis:                  ### Define the optimization objective (single or
                               ### multi-objective)
    - 'power_losses'           ### Real power losses
  which_elements_per_kpi:      ### Define the elements each objective will be
                               ### applied to
    power_losses:
      - 'all'
  kpi_weights:                 ### Define the weights of each objective (for
                               ### multi-objective)
    power_losses: 1

power_flow_config:                  ### Define the power flow configuration
  algo: 'nr'                        ### algorithm that is used to solve
                                    ### the power flow problem.
                                    ### "nr" -> Newton-Raphson
  consider_line_temperature: True   ### If True, net.line must contain a column
                                    ### "temperature_degree_celsius"
  max_iteration: 'auto'             ### maximum number of iterations carried
                                    ### out in the power flow algorithm.
                                    ### 10 for "nr"
  enforce_q_lims: True              ### respect generator reactive power limits
  run_control: False                ### if true, run multiple power flow
                                    ### calculations until all registered
                                    ### controllers are converged

state_config:                    ### Define state variables configuration
  which_states:                  ### Define which state variables to be
                                 ### considered
    - 'bus_voltage'
  which_elements_per_state:      ### Define the elements of which the state
                                 ### selected variables will be applied to
    bus_voltage:
      - 'all'

solver_config:                  ### Define solver configuration
  solver: 'PSO'     ### Define algorithm for solving the problem (PSO for now)
  max_time: 60                  ### maximum time until optimization stops
  stall_iterations: 40          ### Number of iterations since the last change
                                ### in best fitness function value
  swarm_size: 30                ### define population size
  rng_seed: 1                   ### random generated sequence of numbers to
                                ### to initiate the PSO parameters
```

Figure 3.6 Configuration file for the case of real power losses minimization

Optimization algorithm

For the purposes of the present project the particle swarm optimization (PSO) [AD-99] will be used. This method uses a simple mechanism that mimics the formation behavior of birds or fishes swarms so as to guide the particles towards searching optimal global solutions. According to [AD-100] PSO is described by three simple functionalities, separation, alignment and cohesion. The separation refers to the effort of each particle to move away from its neighbors if they are too close. During alignment and cohesion, the particles are move towards the mean direction and position of their neighbors

This project has received funding from the European Union's Horizon 2020 research and innovation programme under grant agreement N°864283

respectively. The equations governing the PSO algorithm are as follows [AD-99], [AD-101]:

$$v_{id}^{t+1} = v_{id}^{t} + c_1 \cdot rand(0,1) \cdot (p_{id}^{t} - x_{id}^{t}) + c_2 \cdot rand(0,1) \cdot (p_{gd}^{t} - x_{id}^{t}), \quad (3)$$

$$x_{id}^{t+1} = x_{id}^{t} + v_{id}^{t+1} \quad (4)$$

The PSO algorithm is comprised by a series of steps depicted below [AD-102], which are also provided in Figure 2-7 as a flowchart:

1. **Initialization for $t = 0$. For each particle**
   a. **the position $\mathbf{x}_{id}^{0}$ is initialized**
   b. **the particle 's optimal position is initialized as its initial position, $\mathbf{p}_{id}^{0} = \mathbf{x}_{id}^{0}$**
   c. **the fitness of each particle is calculated and if $f(\mathbf{x}_{jd}^{0}) \geq f(\mathbf{x}_{id}^{0}) \forall i \neq j$, where f is the objective function, then the global optimal position is initialized as $\mathbf{p}_{gd}^{0} = \mathbf{x}_{jd}^{0}$**
2. **Until a termination criterion to be satisfied, the following steps are repeated for $t = t + 1$:**
   a. **the particle 's velocity is updated, $\mathbf{v}_{id}^{t+1}$ according to equation (3)**
   b. **velocity $\mathbf{v}_{id}^{t+1}$ is compared to the maximum limit of velocity and if found greater, then it is reduced**
   c. **the particle 's position is updated, $\mathbf{x}_{id}^{t+1}$ according to equation (4)**
   d. **the particle 's fitness is calculated $f(\mathbf{x}_{id}^{t+1})$**
   e. **if $f(\mathbf{x}_{id}^{t+1}) \geq f(\mathbf{p}_{id}^{t})$, then the individual optimal position is updated $\mathbf{p}_{id}^{t} = \mathbf{x}_{id}^{t+1}$**
   f. **if $f(\mathbf{x}_{id}^{t+1}) \geq f(\mathbf{p}_{gd}^{t})$, then the global optimal position is updated $\mathbf{p}_{gd}^{t} = \mathbf{x}_{id}^{t+1}$**

This project has received funding from the European Union's Horizon 2020 research and innovation programme under grant agreement N°864283

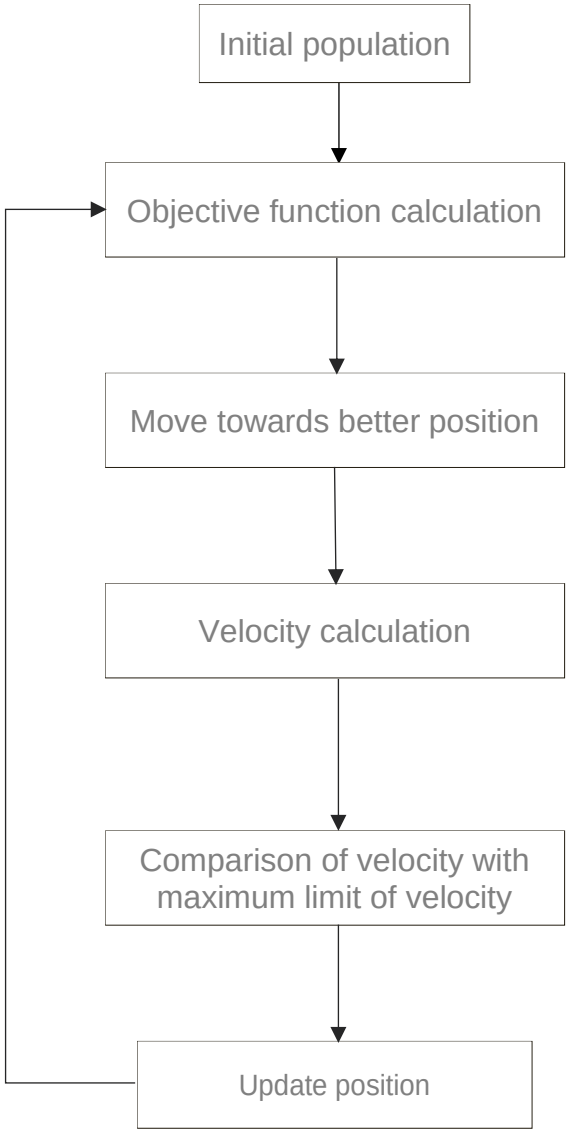

Figure 3.7 Flowchart of PSO algorithm

3.4 Demonstration and Validation

To implement, validate and demonstrate the algorithm three different topologies are applied. These are:

1. **IEEE-123, extended with PV nodes.**
2. **ebalance-plus Resilience Topology (applied on IN-LAB)**
3. **Other Demo-Site (TBC)**

Using the ebalance-plus platform in conjunction with the algorithm shall be demonstrated that:

a) **The algorithm achieves its goals (KPI analysis)**
b) **The algorithm continues to operate correctly when nodes become disconnected / unavailable (ebalance-plus platform benefits demonstration)**

This project has received funding from the European Union's Horizon 2020 research and innovation programme under grant agreement N°864283

The simulation results of Volt/VAr optimization executions for the modified IEEE123 and the ebalance-plus resilience grid topologies are presented in Table 2-1 and Table 2-2 respectively. As stated above, multiple objective functions are taken into consideration, namely voltage violation minimization, real power losses minimization and RES curtailment minimization. In each case, the initial and optimized values of the KPIs are shown. It has to be noted that the voltage deviations are measured as the difference between the grid's buses voltage values and the nominal value which is set to 1 p.u. Looking at these values, it is obvious that the proposed Volt/VAr algorithm achieves its goals.

Topology	IEEE123	
Objective	Voltage violation minimization	Real power losses minimization
KPI initial value	5.213454222917216	3.360886005262138
KPI optimized value	0.7733681334336425	0.1510907405190642

Table 3-1 Simulation results for IEEE123 grid

Topology	ebalance-plus Resilience Topology	
Objective	Voltage violation minimization	Real power losses minimization
KPI initial value	1.5010157447327777	0.00341360723654026
KPI optimized value	0.886436774583558	0.002120340776269087

Table 3-2 Simulation results for ebalance-plus grid

An important metric while trying to optimize an objective is always the speed of convergence. In Figure 3.8, Figure 3.9, Figure 3.10, the convergence of the fitness function values versus the generations of the PSO algorithm are depicted for the cases of RPL, VDM and AP curtailment respectively applied on the IEEE 123 grid. The corresponding graphs for the ebalance-plus grid are shown in Figure 3.11, Figure 3.12 and Figure 3.13.

This project has received funding from the European Union's Horizon 2020 research and innovation programme under grant agreement N°864283

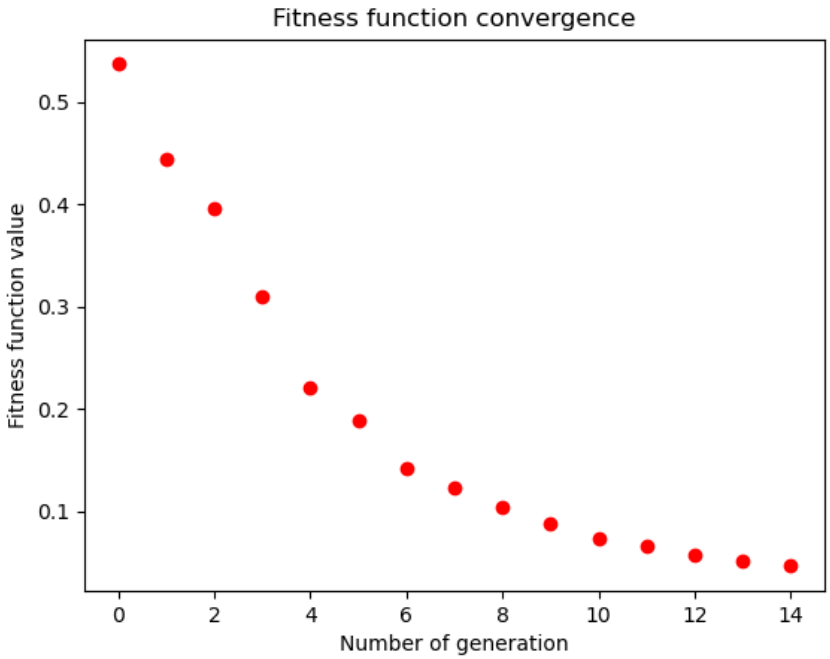

Figure 3.8 Convergence of Power Losses objective for the IEEE 123 grid

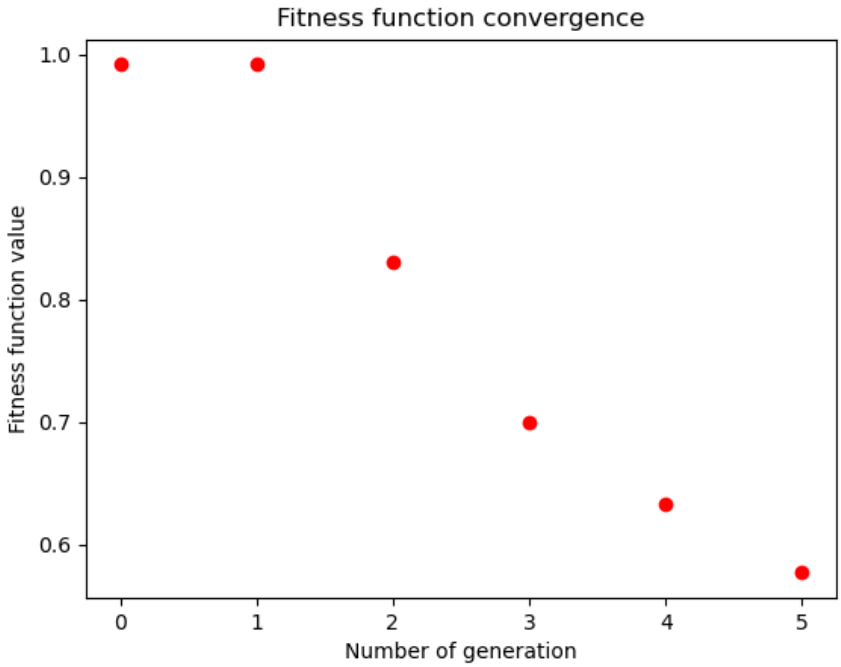

Figure 3.9 Convergence of voltage violation objective for the IEEE 123 grid

This project has received funding from the European Union's Horizon 2020 research and innovation programme under grant agreement N°864283

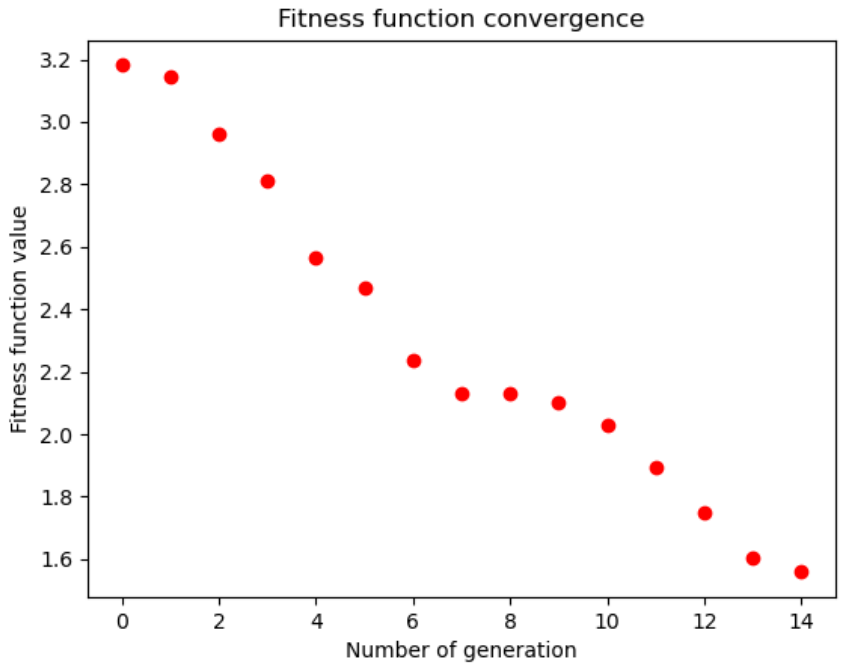

Figure 3.10 Convergence of RES curtailment objective for the IEEE 123 grid

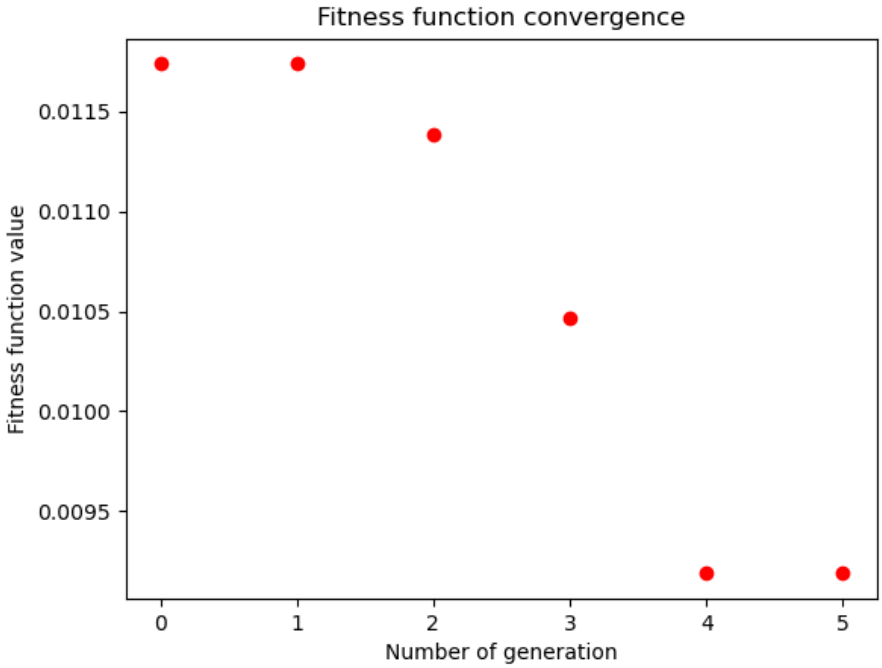

Figure 3.11 Convergence of Power Losses objective for the ebalance-plus grid

This project has received funding from the European Union's Horizon 2020 research and innovation programme under grant agreement N°864283

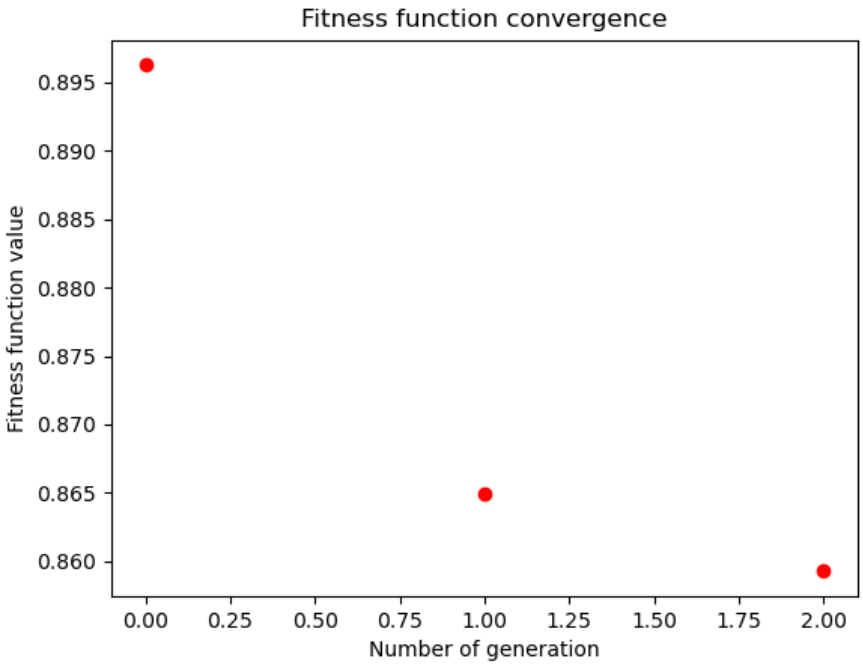

Figure 3.12 Convergence of Voltage Violation objective for the ebalance-plus grid

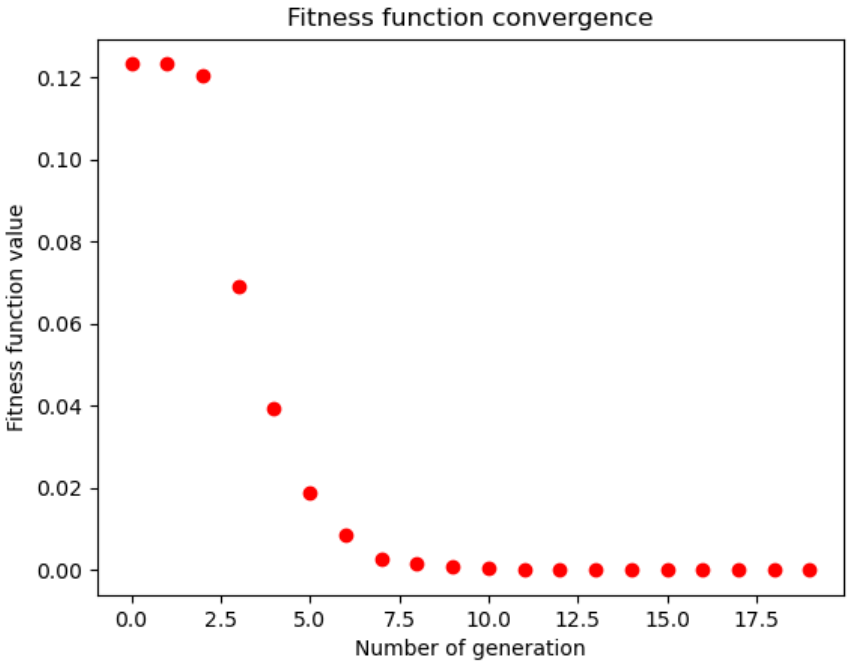

Figure 3.13 Convergence of RES curtailment objective for the ebalance-plus grid

This project has received funding from the European Union's Horizon 2020 research and innovation programme under grant agreement N°864283

4 Monitor power peaks and voltage violation and request support to lower management units

4.1 State of the art

Electrical energy is a product and, like any other product, should satisfy certain requirements in order to maintain a proper quality. All electrical devices require electrical energy, supplied at a voltage that is within a specified range around the nominal value, so that they can operate seamlessly. Therefore, most of the electrical and electronic equipment which is used nowadays requires good voltage quality to avoid deviating from their expected operation.

According to the standard IEC EN 50160 [AD-21] the supplier is the party who provides electricity via a public distribution grid, and the user or customer is the purchaser of that electricity. The quality of power which will be delivered to the user must be ensured by the supplier. However, electrical energy is a product with specific characteristics. The possibility for storing electricity in any significant quantity is very limited, thus most of it is consumed at the instant it is generated. As a result, the quality of the supplied power has to be measured and evaluated at the instant of its consumption. The standard EN 50160 is responsible for setting the proper limits, between which the electric power's quality is acceptable for the uninterrupted operation of the electrical devices of the consumers. The process of maintaining the power quality within those limits is complex, since the supplier and the consumer, whose sensitive electrical equipment is also a source of disturbances, affect the current and voltage waveform of the provided electrical power in a different manner.

When distributed energy resources are included in the electrical grid, the factors which should be taken into consideration, in order to maintain the grid's voltage quality, increase. [AD-22][AD-23]. To begin with, DER units affect the quality of the current and the voltage, as experienced by other users through the grid. Their unique behaviour and their wide-scaled penetration require a detailed assessment of this aspect. Of course, this is not something new. The same problems occur with normal end-user equipment, due to the fast-paced integration of electronics, which has caused an increase to the harmonic levels. The situation is different for DER units for a number of reasons. The most important difference is that the distribution grid is not intended for connecting generator sources. It is the task of the distribution system operator to supply its customers with reliable electricity of little to no deviations from the nominal voltage and frequency values. Additional generator sources connected to the distribution grid often produce unwanted voltage overshoots or drops.

Moreover, the tripping of a DER unit, may have adverse impact on the grid. Specifically, if a large number of DER units trip simultaneously, the grid could become unstable and insecure. In such a scenario, the best practise would be to simultaneously disconnect all the unreliable DER units from the grid as fast as possible, allowing the existing control and protection system of the grid to become more effective in a shorter amount of time. It is very important to consider the design of the DER as well, since it defines

This project has received funding from the European Union's Horizon 2020 research and innovation programme under grant agreement N°864283

whether a unit could handle issues of that type. When the design DER units is optimized for energy production only, ignoring other aspects of the grid to which they are connected, massive DER penetration will undoubtedly cause problems to the voltage quality and grid stability.

It is natural that monitoring and controlling an electrical grid, consisting of multiple elements, each one with a different role, is not a simple task, since large amounts of information are produced, consumed and exchanged among them in real-time. This problem can be solved by creating automatic processes, which handle all the data transactions and implement a common protocol of communication. The FIWARE framework (https://www.fiware.org/) is a tool with such capabilities. It is an open source European initiative and provides open source tools for the next-generation internet. More specifically, it is an open-source platform, consisting of multiple components, which can operate alongside with other third-party platform components, and is used for developing Smart Solutions, such as e.g., Smart Grids, as well as other domains, which are being migrated gradually to the digital world. Moreover, it provides a rather simple yet powerful set of APIs that ease the development of Smart Applications in multiple vertical sectors. The specifications of these APIs are public and royalty-free. Besides, an open-source reference implementation of each of the FIWARE components is publicly available so that multiple FIWARE providers can emerge faster in the market with a low-cost proposition.

4.2 Scope

The scope of this Use Case is to implement an approach for detecting and partially preventing violations of the IEC EN 50160 Voltage Quality Standard, using complex event analysis on the underlying electricity grid, by using cooperatively the ebalance-plus middleware, the management units (MVGMU, LVGMUs and DERMUs) and the FIWARE tools. The main goals of this Use Case are to provide a more reliable and secure electrical grid for the end users, by means of understanding the sources of anomalies, which would then assist the DSO in applying corrective measures, and to demonstrate that complex event analysis can help in conforming with the IEC EN 50160 standard by restricting, and ideally eliminating completely, the unwanted effects of the DER units on voltage quality.

The aim is the application of the aforementioned Voltage Quality Standard in Voltage Quality Assurance (VQA) in a distributed manner, for an electrical power distribution grid, given a specific topology, in order to apply and demonstrate concepts and technologies of the ebalance-plus project. One core scenario is taken into consideration, towards the demonstration of a few key aspects. The first one is the constant monitoring at primary and secondary substations via MUs equipped with power analysers, followed by the use of historic and real time data to detect any deviations from the IEC EN 50160 standard and to generate statistical limits. Two more are the combinatorial analysis of events and metrics in order to determine any violations of the IEC EN 50160 standard and to indicate correlations with certain behaviours of the grid's elements (e.g. DER), as well as the application of Volt-VAr Optimisation (VVO) as a partially reactive measure.

The EN-50160 standard defines the supply voltage characteristics for Power Grids under normal operation. To achieve its goals the standard sets forth a series of

This project has received funding from the European Union's Horizon 2020 research and innovation programme under grant agreement N°864283

compliance and statistical thresholds that need to be observed. To apply the standard and especially its statistical thresholds, it is necessary to assess a series of metrics (most notably V, P, Q, f) in a historical context. However, by leveraging the current framework it is possible to prevent violations by analyzing events on the power grid as they occur. These events include but are not limited to, set-point modification of DER and capacitor and TAP state changes. By analyzing these primary events it is possible to determine correlations that can lead to loss of power-quality. Specifically, the events are correlated both among themselves (one event leads to another) and versus the available metrics (an event leads to voltage drop/rise or frequency change).

Such events can be assessed macroscopically in time and provide useful insights to operators to help them understand how different actions or series of actions can lead to disruption of voltage quality according to the standard. This creates the opportunity of creating a proactive approach in the application of the standard thus ensuring a larger degree of compliance.

Based on the above the application of the standard can have two forms. A reactive approach where monitoring and historical data are used for measuring compliance and a proactive approach where complex event analysis is used to avoid violations in the first place. In any case, event and metric monitoring will occur on all levels of the grid with the use of the appropriate MUs (DERMU, MVGMU, LVGMU) and power quality analysis, while the assessment of the information will take place on the MVGMU level. To perform its goal, the algorithm of the MVGMU component will be responsible for the synthesis of primary events with metrics based on both real time and historic data.

4.3 Technical Methodology

First of all, it is crucial to define the topology of the electrical grid which will be used, as described in chapter 3.3.1. This is a crucial step, since it dictates how each one of the required MUs (MVGMU, LVGMUs and DERMUs) will be deployed on the appropriate nodes of the grid.

After the deployment of the MUs, the qualities that will be monitored and measured should be defined and the monitoring process will start. When monitoring these qualities, the measured data and the events that occur will be constantly stored, creating a historic database. The monitoring and storing processes will be achieved through the ebalance-plus framework, since it will enable the communication between the MUs of the grid.

At the same time, any events generated during this phase will be sent to the Complex Event Processor (CEP) (https://fimac.m-iti.org/3e.php), which is deployed on the server's side of the FIWARE framework, and will be examined analytically, in order to find any possible correlations between them. The CEP toolbox fits very well to this task, because it can track a series of events and trigger actions, based on preset conditions. The CEP analyses data of events in real-time, provides instant insight and responds immediately to changing conditions. In contrast to most standard reactive applications, which are designed to react to single events, the CEP is designed to react to certain situations. The term "situation" refers to a condition that is based on a sequence of events which take place within a dynamic time window, called processing context. Situations include composite events (e.g., sequence), counting operators on

This project has received funding from the European Union's Horizon 2020 research and innovation programme under grant agreement N°864283

events (e.g., aggregation) and absence operators. As a result, the features and capabilities of CEP form a powerful utility, able to define, adjust and maintain the event processing logic of the application, while at the same time it is designed to meet both the functional and nonfunctional requirements, without diminishing the performance of the application.

Finally, any violations found, according to the IEC EN 50160 standard, will be reported, with the ultimate goal to react via optimization of the Volt/VAr algorithm, if any number of DERs were associated with the violation, and restore the grid's power quality within the acceptable limits. A complete table of the IEC EN 50160 standard specifications is presented in Table 4-1 Specifications of the IEC EN 50160 standard. Table 4-1. Afterwards, the monitoring process will go on, until a new voltage violation is found, analysis and the appropriate actions (if any) take place, creating a continuous execution loop. A complete flowchart of the process described above is presented in Figure 4.2.

The producers of the events will be the MVGMU, LVGMUs and DERMUs, with specific definitions and specifications, related to the FIWARE technology. These events shall be processed by the CEP in real-time, in order to immediately obtain information about their nature, origin and severity. Thus, the CEP in our case will be used for its exhaustive meta-model definition for event classification and real-time insights generation whenever an event associated with voltage quality violation is triggered; two aspects which we believe that elevate the ebalance-plus platform with a common European Standard. A conceptual diagram of the methodology described in the previous paragraphs is shown in Figure 4.1.

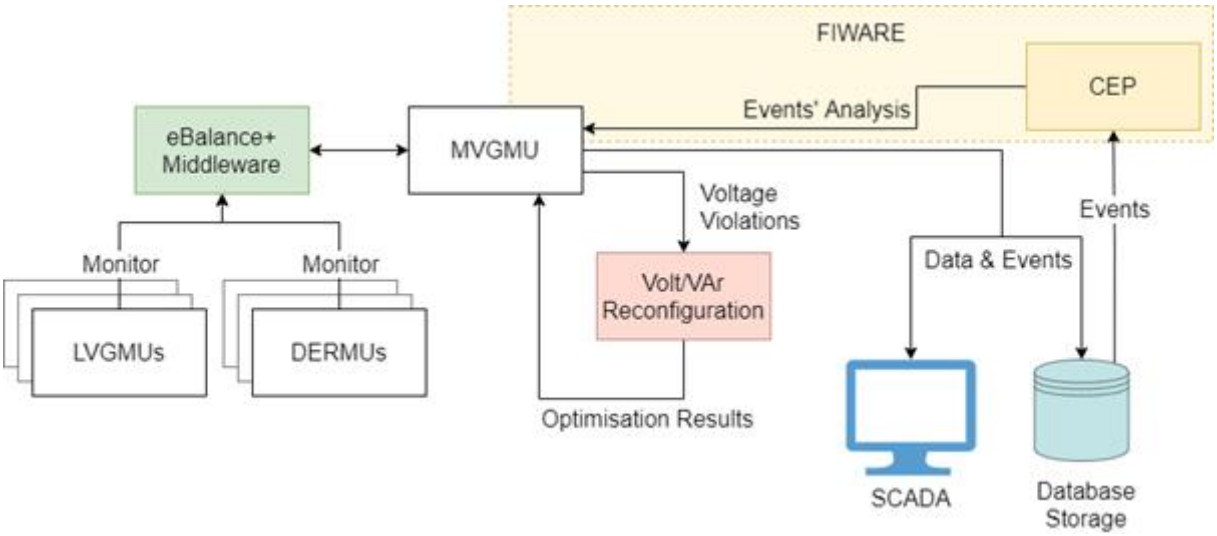

Figure 4.1 Conceptual diagram of the monitoring, event processing and VVO reconfiguration operations.

Parameter	Supply voltage characteristics according to EN 50160
Power frequency	LV, MV: mean value of fundamental measured over 10 s ±1% (49.5 - 50.5 Hz) for 99.5% of week -6% … +4% (47- 52 Hz) for 100% of week
Voltage magnitude variations	LV, MV: ±10% for 95% of week, mean 10 minutes rms values

This project has received funding from the European Union's Horizon 2020 research and innovation programme under grant agreement N°864283

Rapid voltage changes	LV: 5% normal 10% infrequently $P_{lt} \leqslant 1$ for 95% of week MV: 4% normal 6% infrequently $P_{lt} \leqslant 1$ for 95% of week
Supply voltage dips	Majority: duration <1s, depth <60%. Locally limited dips caused by load switching on: LV: 10 - 50%, MV: 10 - 15%
Short interruptions of supply voltage	LV, MV: (up to 3 minutes) few 10s - few 100s incidences per year Duration < 1 s, 70% of them.
Long interruption of supply voltage	LV, MV: (longer than 3 minutes) <10 - 50 incidences per year
Temporary, power frequency overvoltages	LV: <1.5 kV rms MV: 1.7 U_c (solid or impedance earth) 2.0 U_c (unearthed or resonant earth)
Transient overvoltages	LV: generally < 6kV, occasionally higher; Rise time: ms - µs. MV: not defined
Supply voltage unbalance	LV, MV: up to 2% for 95% of the monitoring week 10min-average values
Harmonic voltage	See Table 4-2
Total Harmonic Distortion	THD < 8% U_n

Table 4-1 Specifications of the IEC EN 50160 standard.

Odd harmonics				**Even harmonics**	
Not multiples of 3		**Multiples of 3**			
Order	**Relative voltage (%)**	**Order**	**Relative voltage (%)**	**Order**	**Relative voltage (%)**
5	6	3	5	2	2
7	5	9	1.5	4	1
11	3.5	15	0.5	6 … 24	0.5
13	3	21	0.5		
17	2				
19	1.5				
23	1.5				
25	1.5				

Table 4-2 Limit values of individual harmonic voltages at the supply terminals for orders up to 25, given in percent of the nominal voltage U_n.

This project has received funding from the European Union's Horizon 2020 research and innovation programme under grant agreement N°864283

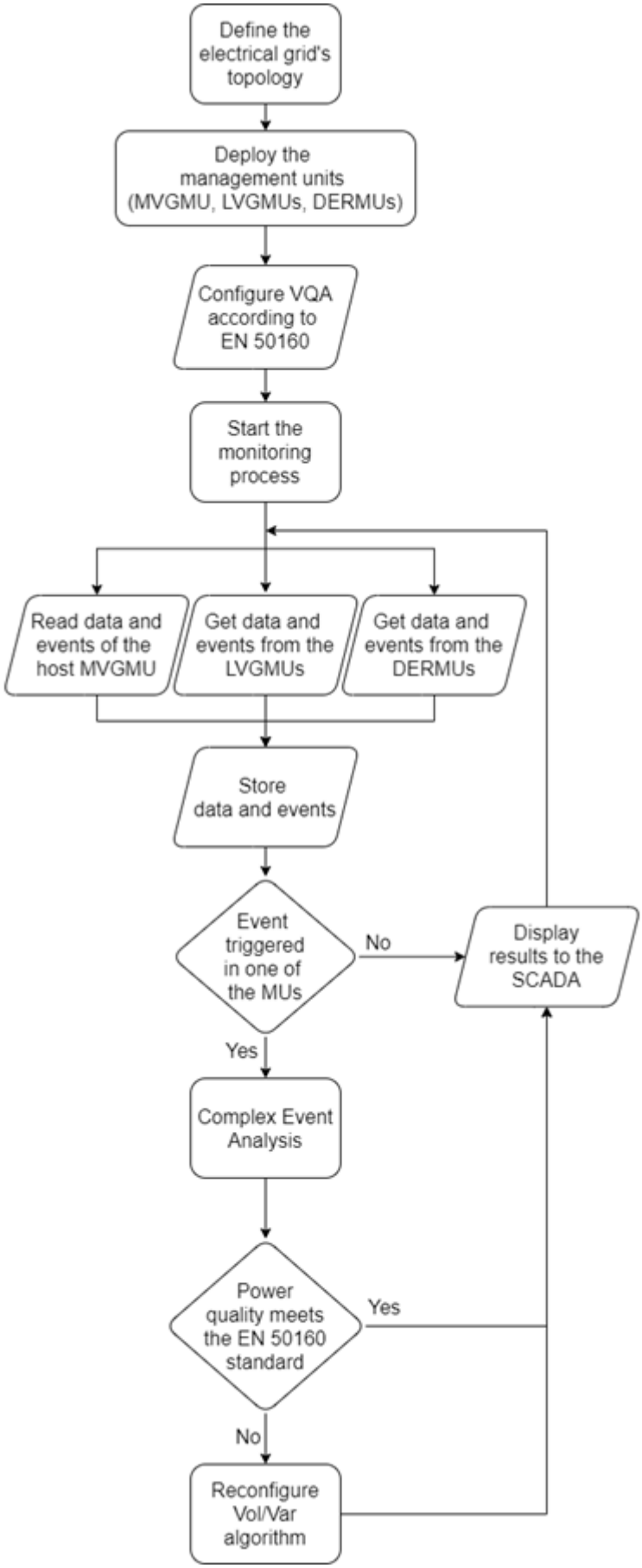

Figure 4.2 Flowchart of power peaks and voltage violations monitoring followed by the reconfiguration of the Volt/Var algorithm.

This project has received funding from the European Union's Horizon 2020 research and innovation programme under grant agreement N°864283

4.4 Demonstration

According to the use case previously described, two scenarios will be demonstrated. The topology which will be used in both scenarios will be the IEEE 123-bus system. Moreover, in both scenarios the monitoring will take place on a LVGMU, which will be simulated by a programmable AC generator, alongside with a power quality assurance device attached to its output and a management unit, which will provide the monitored data to the MVGMU.

The AC generator will be producing signals according to the parameters given by the user, which will allow the injection of disturbances in the power quality, e.g. voltage peaks or drops. The power quality assurance device will be constantly reading the values of the voltage, the current and the frequency and calculating the active and reactive power. The management unit will be sending those values to the MVGMU for storage, display to the SCADA and further analysis. If any deviations from the EN 50160 standard are found, the MVGMU will generate the relevant events. Additionally, any changes in the state of the grid's elements (e.g. a DERMU disconnects from the grid) will produce a corresponding event. All events will have information about the cause that created them, a unique id, a timestamp and a geolocation when applicable.

Afterwards, the CEP will retrieve these events, attempt to find an association between them during a given time window, and report the results back to the MVGMU. This operation will be available after an initial time period from the deployment of the management units, because it will be based on the identification of certain patterns, specific to the examined grid topology (e.g. the tripping of certain DERMUs lead to voltage drops in a certain LVGMU). Finally, the MVGMU will provide these results to the Volt/VAr optimisation algorithm, which will make the required adjustments, in order to maintain the stability of the grid.

In the first scenario, the tripping of multiple DERs at the same time will be simulated. This would cause a power shortage, leading to a voltage drop in the LVGMU where the DERs are connected. In the second scenario, the connection of multiple DERs at the same time will be simulated. This would cause a power increase in the LVGMU, leading to a voltage peak.
The expected result is to detect those voltage violations, by continuously monitoring the LVGMU, and attempt to find the issue that caused them by feeding the relevant events to the CEP of the FIWARE framework. Afterwards, these finding can be used to request a reconfiguration of the VVO algorithm. As a result, the aims of both scenarios are to:

- **Create an event when a DER disconnects from/connects to the grid.**
- **Create an event when the voltage drops/rises in the LVGMU.**
- **Send the events to the MVGMU.**
- **Detect the voltage violation.**
- **Find the root of the violation, by associating the generated events.**
- **Request a reconfiguration of the VVO.**

This project has received funding from the European Union's Horizon 2020 research and innovation programme under grant agreement N°864283

5 Fault Detection Isolation & Restoration – FDIR

5.1 State of the art

It is a fact that modern electricity distribution networks are plagued by multiple types of faults such as line tripping, relay faults, transformer faults etc. [AD-40], [AD-41], causing electricity interruptions with severe economic consequences ranging from production loss and restart costs to equipment damage, and raw material spoilage [AD-42]. In trying to cope with these phenomena, the utilities have come up with FDIR procedures which are key building blocks for the self-healing capability of a utility's future advanced distribution management system (DMS) [AD-43]. Several reviews can be found in the literature including FDIR trends and challenges [AD-44], fault management in microgrids [AD-45] and restoration of smart grids [AD-46].

Most of the published work has considered the two stages of FDIR independently [AD-47]. Typical distribution systems have normally closed sectionalizing switches and normally open tie switches (i.e., to interconnect feeders and allow load transfer among them). During the first stage, a fault is detected, and then it must be located and isolated as quickly as possible. Fault detection is to discover that a fault has occurred even if the root cause is not known yet. Faults may be detected by alarms based on high currents and/or low voltages. For example, when a fault occurs, feeder circuit breakers (FCBs) trip when a current exceeds a pre- determined value. Once the fault has been detected, the smallest possible part of the system is isolated by opening the first upstream and downstream switches from the fault to isolate the fault from both directions. As soon as the faulty section is isolated, the upstream out-of-service loads are restored through closing of the FCB. In order to determine whether service restoration from neighboring healthy feeders is possible, a capability estimation is carried out. Then follows the second stage where, the restoration plan starts to restore power delivery to the affected customers beyond the faulted zone by transferring them to other supporting feeders using tie switches [AD-48].

Although, a self-healing grid minimizes customer minutes lost (CML), system average interruption duration index (SAIDI) and average outage duration [AD-49], serious challenges emerge when employed.

From a technical aspect, the employment of modern technologies that provide data acquisition, decision-support systems, dynamic power flow control as well as the integration of digital signal processing techniques, would yield to more effective and reliable self-healing systems. A countable amount of research has been reported towards these issues, paving the way for more advanced and successful FDIR schemes [AD-50], [AD-51]-[AD-53], [AD-83]-[AD-85].

From a methodological point of view, FDIR can be implemented adopting two different control strategies, centralized and decentralized/distributed. A central optimization solver reads all the system data and then processes them in order to obtain a solution [AD-47]. Although a centralized control may confine the best solution to the problem, it requires a large amount of data management and thus a high computational burden.

This project has received funding from the European Union's Horizon 2020 research and innovation programme under grant agreement N°864283

Decentralized approaches focus mostly on parallelizing the solution of a problem. The control/protection action is taken within each distribution or primary substation and the whole system behavior is the collection of these individual actions.

Currently, one main issue that utilities face is the lack for meters and sensors in distribution networks. Therefore, a lot of research was done to develop fault location algorithms and include sending a repair crew to localize a fault and then fix the problem [AD-55], measuring the apparent impedance [AD-56], carrying out three-phase circuit analysis [AD-57], [AD-58], or integrating artificial intelligence in analyzing power quality data [AD-59]-[AD-61] or travelling waves of the captured signals during fault [AD-62]-[AD-64]. To overcome the multiple disadvantages of centralized control based methods [AD-65], [AD-66] several automatic fault location detection and isolation algorithms based on Modal Analysis (MAS) have been proposed to enhance the reliability, survivability, availability, and efficiency of power systems [AD-67].

Many approaches have been proposed to address SR problems in a centralized way, including heuristics [AD-68]-[AD-71], expert systems [AD-72]-[AD-74], meta-heuristics [AD-75]-[AD-77], and mathematical programming [AD-78], [AD-79]. The main drawbacks of the centralized methods are summarized in high computational time and maintenance cost, non-guarantee of optimal solution and algorithmic complexity. Therefore, the intelligence and control should be distributed at every component level, as is performed in MAS that contains multiple computing elements as agents [AD-80]-[AD-82].

When designing FDIR procedures the impact of RES penetration in distribution networks should definitely be taken into account. One of the main challenges in incorporating renewable energy DGs in SR plans as supporting sources is their variable and uncertain environment. A review of the literature shows that most of the published work has considered only dispatchable DG units, with a few studies including the effect of renewable resources associated with the restoration problem [AD-54], [AD-86]-[AD-88].

To summarize, in order to realize the concept of the self-healing grid, future research directions should focus on filling the gaps in the following challenges:

- Infrastructure for a self-healing grid in terms of IT related enhancements, dynamic analysis, data acquisition, maintenance, and monitoring and control actions.
- Developing decision support tools that are characterized by flexibility and distributed applicability.
- Handling of RES intermittency and uncertainty.
- Load forecasting integration so as to allow more accurate and realistic decision making.

5.2 Scope

The FDIR function is usually solved and implemented under emergency conditions. Moreover, it is a computationally complex problem [AD-89] because it is 1) combinatorial due to the large number of switching elements; 2) nonlinear because of the nonlinear nature of power flow constraints; 3) non- differentiable because any change in a switch status may change the values of objectives and/or constraints; 4) constrained because of the radiality and the operational voltage and current restrictions; and 5) multi-objective.

This project has received funding from the European Union's Horizon 2020 research and innovation programme under grant agreement N°864283

The most common objective functions are listed below.

- Maximization of load restored

$$\sum_{i=1}^{m} \frac{\int_{T_i}^{T_{total}} P_i^{load}(t)dt}{T_{total}}$$

where T_{total} is the total restoration time, T_i is the i-th restoration stage time period and $P_i^{load}(t)$ represents the restored load at stage i.

- Minimization of restored time

$$\sum_{t=1}^{T} \sum_{i=1}^{N} C_{t,i} max\left(X_{t,i} - X_{t-1,i}, 0\right)$$

Where ???

- Minimization of restoration cost

$$\sum_{i=1}^{N-1} C_{SW}(i, i+1) + \sum_{tr=1}^{N_{TR}} C_{TLoL}(L_{tr}^{st}) + \sum_{i=1}^{N} C_{PP,i}^{st} + \sum_{i=1}^{N} C_{CI,i}^{st}$$

where C_{SW} is the switching cost, C_{PP}^{st} and C_{CI}^{st} respectively refer to the total cost of purchasing power from the substation and total customer interruption cost and $C_{TLoL}(L_{tr}^{st})$ calculates the total cost of transformer loss of life for all N_{TR} transformers of the network in which L_{tr}^{st} is a $1 \times N$ matrix comprising the tr-th transformer load in all intervals of the period under study.

- Maximization of reliability

$$SAIFI = \frac{\sum_{i=1}^{M} N_i}{N_T}$$

where N_i and N_T are the number of interrupted customers for each sustained interruption event during the reporting period and the total number of customers served for the area respectively.

$$SAIDI = \frac{\sum_{i=1}^{M} r_i N_i}{N_T}$$

where r_i is the restoration time for each interruption event.

5.3 Technical Methodology

In this section the technical details of the present FDIR procedure are described. As with the rest of the use cases, a configuration is needed. For the FDIR purposes, this file comprises of the grid's topology (Figure 2-4), the failure information (Figure 4-4), the objective function, the use case scenario, the communication graph between the nodes, the set of possible subgrids (Figure 4-4) and the MU-subgrids combinations. Then, according to these combinations and using the grid's state, multiple solutions are obtained by executing optimal power flow for each subgrid and finally the best solution is selected. The flowchart of this procedure is depicted in Figure 4-1. The high-level architecture of the algorithm in terms of inputs and outputs is depicted in Figure 4-2. As can be seen the inputs are comprised of the grid's topology, the execution period, the optimization objective, the network's real time state, the information about the failures and finally the MU configuration block which contains the communication

This project has received funding from the European Union's Horizon 2020 research and innovation programme under grant agreement N°864283

protocol among the MUs. The outputs are divided in P/S related assets (TAP, CAP), S/S assets (capacitor state, voltage level) and DER assets (DER P and Q setpoints). The FDIR scheme is given in Figure 4-3 where all the individual components of the algorithmic frame are provided. All the functionalities are controlled by the Controller block. The core part is optimization scheme where the FDIR optimization takes place. The achieved KPIs are managed by the KPI analyzer.

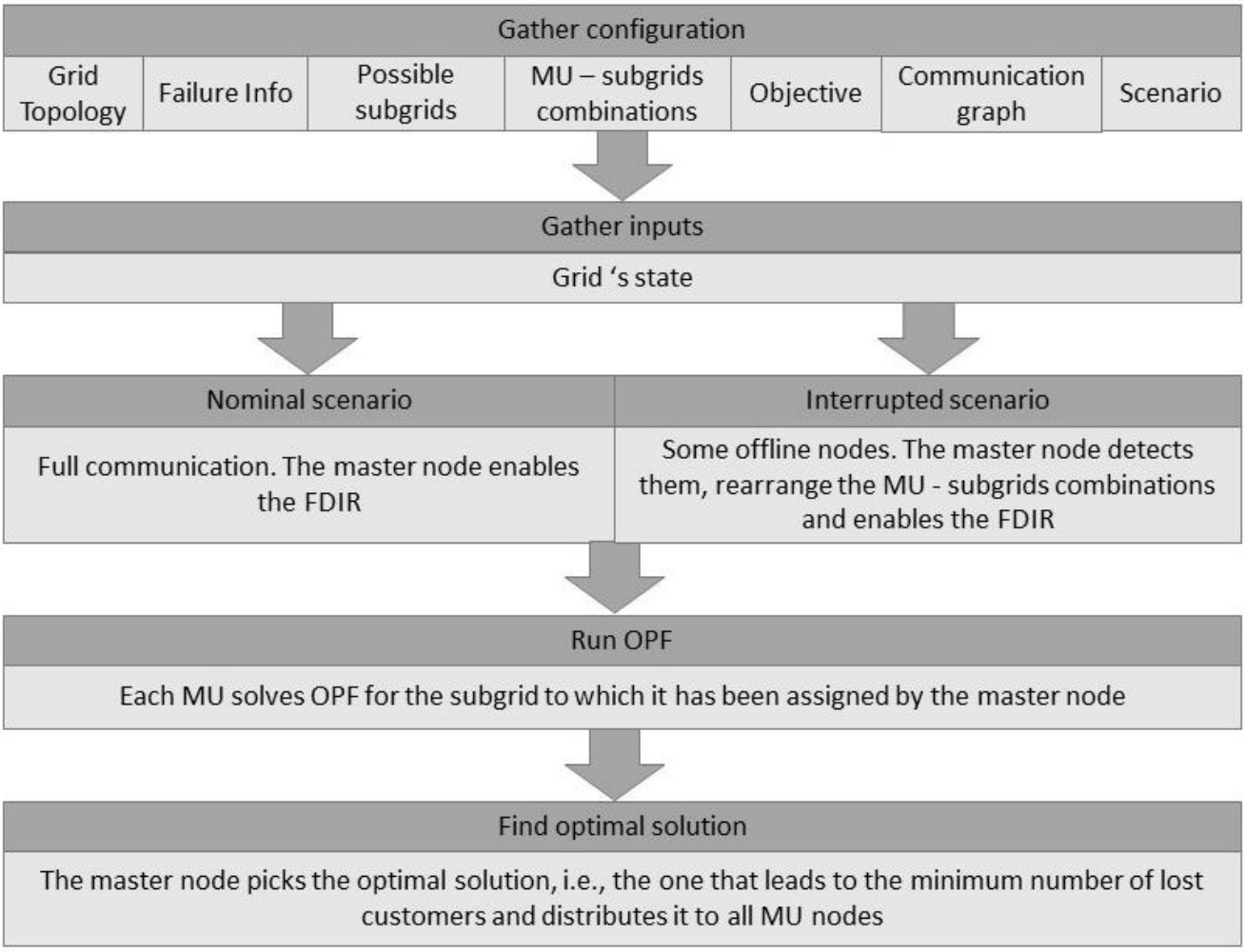

Figure 4-1 FDIR execution process

This project has received funding from the European Union's Horizon 2020 research and innovation programme under grant agreement N°864283

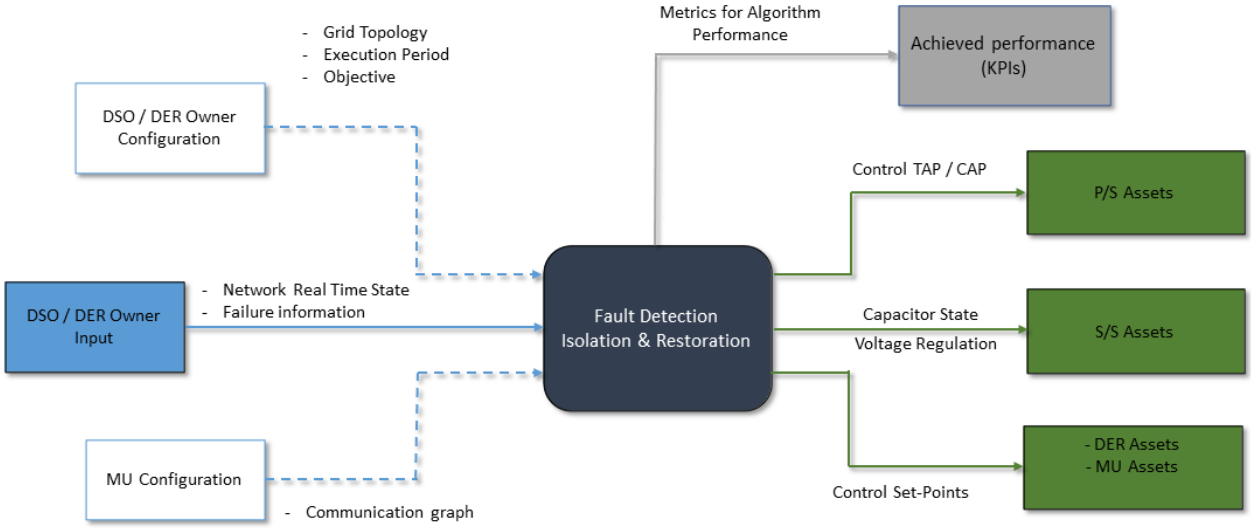

Figure 4-2 High-level block-diagram for FDIR algorithm

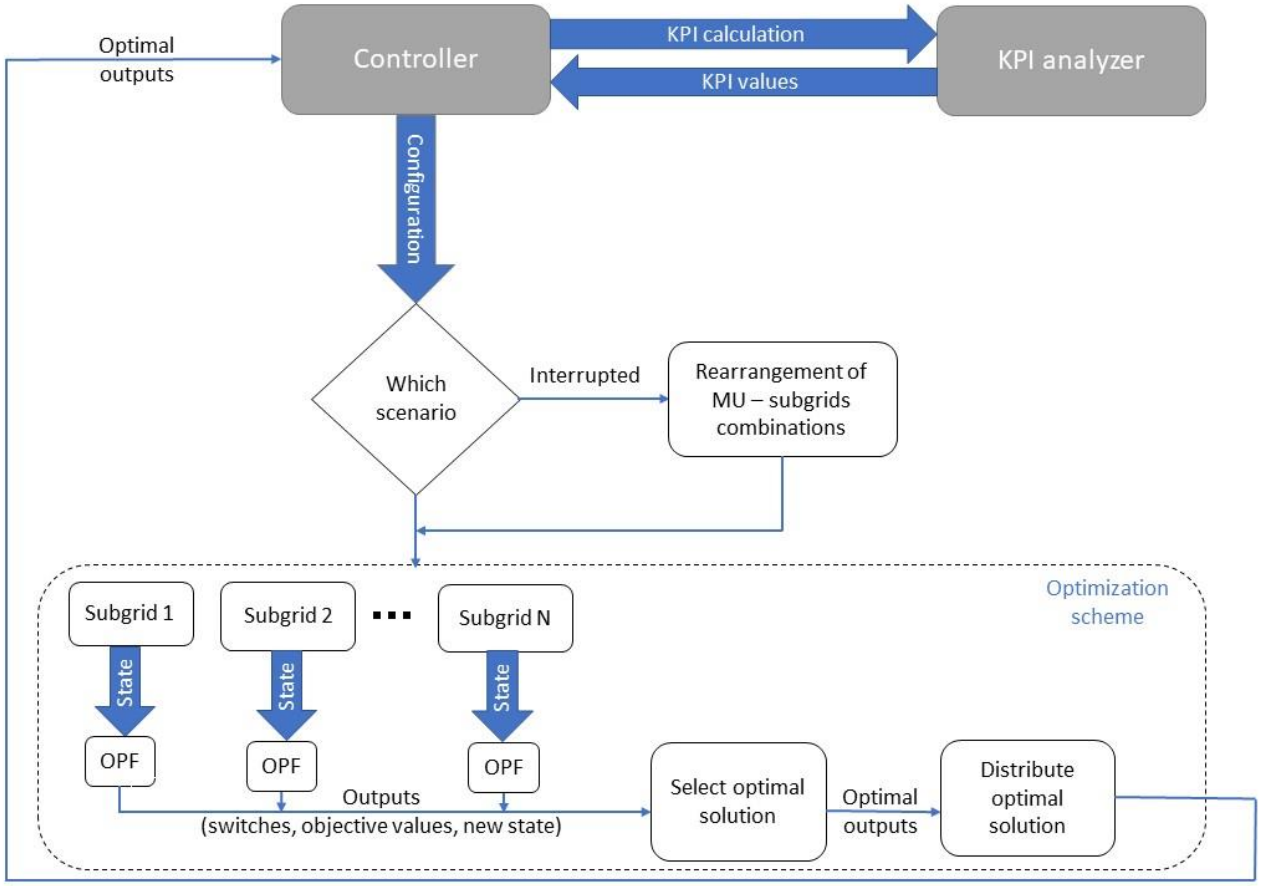

Figure 4-3 FDIR scheme

This project has received funding from the European Union's Horizon 2020 research and innovation programme under grant agreement N°864283

```
fdir_config:
  Fault:
    - name: "Fault_1"
      type: "relay_fault"
      location: "line 5"
  Formations:
    - name: "Formation_1"
      switches: [{name: "SW_3", closed: False}, {name: "SW_5", closed: True},
{name: "SW_13", closed: True}]
    - name: "Formation_2"
      switches: [{name: "SW_3", closed: False}, {name: "SW_9", closed: True},
{name: "SW_14", closed: True}]
    - name: "Formation_3"
      switches: [{name: "SW_3", closed: False}, {name: "SW_12", closed: True},
{name: "SW_15", closed: True}]
    - name: "Formation_4"
      switches: [{name: "SW_3", closed: False}, {name: "SW_5", closed: True},
{name: "SW_13", closed: True},
                 {name: "SW_9", closed: True}, {name: "SW_14", closed: True}]
    - name: "Formation_5"
      switches: [{name: "SW_3", closed: False}, {name: "SW_5", closed: True},
{name: "SW_13", closed: True},
                 {name: "SW_12", closed: True}, {name: "SW_15", closed: True}]
    - name: "Formation_6"
      switches: [{name: "SW_3", closed: False}, {name: "SW_9", closed: True},
{name: "SW_14", closed: True},
                 {name: "SW_12", closed: True}, {name: "SW_15", closed: True}]
```

Figure 4-4. FDIR configuration example for a random fault and the respective possible formations

5.4 Demonstration

Apply the scenarios discussed in the Use Case definition document on eBalance Resilience Topology (applied on IN-LAB)

Using the ebalance-plus platform in conjunction with the algorithm shall be demonstrated that:

c. **The algorithm achieves its goals (KPI analysis)**
d. **The algorithm continues to operate correctly when nodes become disconnected / unavailable (ebalance-plus platform benefits demonstration)**

For demonstration purposes, a random case is specified and examined following the steps below.

1) Assumption: All switches are closed except 5, 9, 12, 13, 14 and 15.
2) Specify fault: Failure in line 5 leads to opening of switch 3
3) Specify all switches configurations that are likely to give feasible solutions.
    a. close switch 5 and 13
    b. close switch 9 and 14
    c. close switch 12 and 15
    d. close switch 5, 9, 13 and 14
    e. close switches 5, 12, 13, and 15
    f. close switches 9, 12, 14 and 15

This project has received funding from the European Union's Horizon 2020 research and innovation programme under grant agreement N°864283

These 6 possible configurations compose 6 different OPF problems.

4) Assign each problem to 3 different LVGMU nodes in a random way. There are 6 LVGMU nodes so each one will solve 3 problems.
   Suppose that after the assignment, the following solutions have been obtained.
   $S_{11}, S_{13}, S_{15}, S_{22}, S_{24}, S_{21}, S_{36}, S_{32}, S_{34}, S_{43}, S_{46}, S_{41}, S_{53}, S_{54}, S_{55}, S_{62}, S_{66}, S_{65}$
   where S_{ij} represents the solution of the i-th problem by the j-th node.
5) In a full communication scenario the 3 solutions of the same problem must agree, there is no reason to solve the problem 3 times, but when there is interrupted communication, then we obtain the solution from the on-line nodes. Suppose that the solutions for each problem are as follows.
   $S_{13}, S_{21}, S_{32}, S_{43}, S_{55}, S_{65}$
6) Among these solutions the one that leads to the maximum number of customers served, is selected. Suppose that the final solution is S_{13}.

6 Simulation of intentional islanding and load shedding after cascading failures

6.1 State of the art

Intentional islanding is the purposeful sectionalisation of the utility system during widespread disturbances to create power "islands". These islands can be designed to maintain a continuous supply of power during disturbances of the main distribution grid. The distributed energy resources can then supply the load power demand of the islands created until reconnection with the main utility system occurs.

A Cascading Failure (CF) is defined as a sequence of dependent failures of individual components that successively weakens the power system and could result in electrical instability and large-scale blackouts and they originate from strong interdependencies inside the grid. Massive economic and social impacts of such events have motivated a great deal of research effort on studying the vulnerability of the power grids to CFs [AD-27], [AD-28]. Transmission line overload due to contingency is the most common initial cause of CFs in power systems.

This project has received funding from the European Union's Horizon 2020 research and innovation programme under grant agreement N°864283

Other faults that appear during cascading failures incidents are:

1. Loss of power on power line (transient fault)
2. Voltage drop in electrical power supply (brownout)
    a) Drop of wind speed on Wind Farms (WF)
    b) Heavy cloud on PV plants
    c) Faulty panel/array on PV plants
    d) Fault on diesel generator
3. Blackout from tripping power stations
4. Rolling blackout when electricity demand exceeds supply
5. Frequency drop

During the CF the state of the system transits from one state to another state as the lines get tripped. This transition is usually shown by the state graph. The state graph shows all possible states for a system. It also shows the probability of transitions from one state to the other. One way to model the CFs is based on the markovian approach where the power system is analysed based on the state of its components such as transmission lines and transformers [AD-29].

When addressing cascading failures, it is necessary to develop a simulation model in order to investigate different aspects of this phenomenon, to reveal the weakness of the grid and potentially recommend remedial actions. There exist two major approaches in simulating CF including dynamic transient models [AD-30], [AD-31] and quasi-steady state (QSS) models [AD-32], [AD-33] each have advantages and disadvantages.

In the dynamic models, the dynamic components, such as rotating machines, exciters, and governors, as well as all protective components of the system along with their dynamic behaviour, are modelled using differential equations. The computational burden and numerical failure in solving differential equations are disadvantages of these models.

QSS models rely on the steady-state assumption for the system where the flow re-dispatch of the network is calculated based on power flow (PF) analysis. The main difference among QSS models is the choice of the PF model they incorporate in their simulation. Most of the QSS models use DC approximation due to its fast and guaranteed convergence to calculate redistribution of power flow after line trips. However, this comes at the expense of assuming flat profiles for voltage and thus being unable to capture voltage-related failures. Full ACPF is also incorporated in several QSS models however, the convergence of ACPF is a challenging issue especially when many lines go offline during the escalation of CF.

A cascade failure simulator (CFS) shall be able to simulate various cascade failure models such as: Line tripping by over-current, Distance and temperature relays, Under-voltage load shedding, Under-frequency load shedding. A mechanism that triggers one or more faults should also exist.

Successive line tripping during the escalation phase of CF usually causes the formation of several islands in the power network. Intentional islanding is a condition in which a distributed generation source continues to supply power to the local loads

This project has received funding from the European Union's Horizon 2020 research and innovation programme under grant agreement N°864283

during a catastrophic utility failure. In this framework an island detection algorithm is used after each trip to identify newly formed islands [AD-34]. The island will remain operational for a long time if the DG alone can meet the local load demand. This may interfere with the recloser system, protection co-ordination and can even lead to hazards. Consequently, the disconnection of the DG system from the grid is required when islanding is detected. Also controlled islanding can improve the reliability of the power system considerably [AD-35], [AD-36], [AD-37].

To implement a successful intentional island, the system should detect the islanding event as soon as the grid gets disconnected. An efficient islanding detection algorithm is needed for this task. These algorithms can be broadly classified as local methods and remote methods [AD-38], [AD-39]. Remote methods are based on the communication between local DG and the utility grid whereas local methods rely on monitoring parameters like voltage and frequency at the DG site. In grid connected mode, DG should provide constant active and reactive power to the system. The voltage and frequency at the point of common coupling (PCC) are dictated by the grid. In autonomous or islanded mode, the aforementioned conventional current controlled strategy is not suitable, as there is no grid to maintain the voltage and frequency at the PCC. Hence when grid is disconnected, the interface controller should be switched to a voltage control mode. The switching between two modes depends on load generation mismatch. However, the system may not be able to sustain an island due to the excessive variation of frequency and voltage. Hence, when the required demand is more, some load should be cut off using an efficient load shedding scheme, to prevent the voltage and frequency collapse.

Cascading failures comprise of a critical challenge in supply networks such as electric power grids, while they could lead to major economical and functional issues. The above supervision/control scheme can be used to address cascading failures and increase the network resilience and stability.

6.2 Scope

The aim of intentional islanding within the proposed approach is the resiliency of the network in terms of frequency balancing and continuous demand supply. This optimization task is conceptualized by executing Optimal Power Flow for several islanding setups of the network. The problem formulation includes the objective of load shedding and switches cost minimization as described in (eq. 5.1).

$$IC = N \times SC + \sum_{i=1}^{I} L_i \times LC \times T_i \quad (5.1)$$

Where N, is the total number of switches, SC is the cost per switch, I is the number of shedded loads, L_i is the i-th shedded load amount, LC is the load shedding cost per kW and T_i is the duration that the i-th load is cut-off. IC (Islanding Cost) is the total cost of switches plus the total cost of shedded loads.

The design variables comprise of the set-points of DERs while the constraints of the Intentional islanding problem are given below:

- Node voltage limits
- Transformer constraints

This project has received funding from the European Union's Horizon 2020 research and innovation programme under grant agreement N°864283

- Transformer tap constraints
- Line loading limits
- Slack bus (battery) active and reactive power injection limits
- Distributed generation limits
- Upper and lower limits of the curtailed power of each RES unit
- Upper and lower limits of the reactive power of PV inverters

6.3 Technical Methodology

The technical details of the intentional islanding procedure are provided in this section. First of all, a configuration that contains the network's topology, the optimization objectives, the type and point of failure (e.g., line tripping) that enables the islanding, as well as all the possible islanding setups, has to be defined. Then, the current state of each island is needed as input to the OPF algorithm which has already been described. The aim of this process is to extract the islanding setup with the minimum cost, leading to the minimization of customers without power supply. The effectiveness of the algorithmic framework can be measured by SAIDI (System Average Interruption Duration Index) and SAIFI (System Average Interruption Frequency Index) indices. Finally, the load level of the islands is monitored continuously, and load shedding is applied in case of power imbalance. The high-level algorithmic scheme is depicted in Figure 5-1. In Figure 5-2, a flowchart of the proposed algorithm is provided, while the integrated optimization scheme is depicted in Figure 5-3.

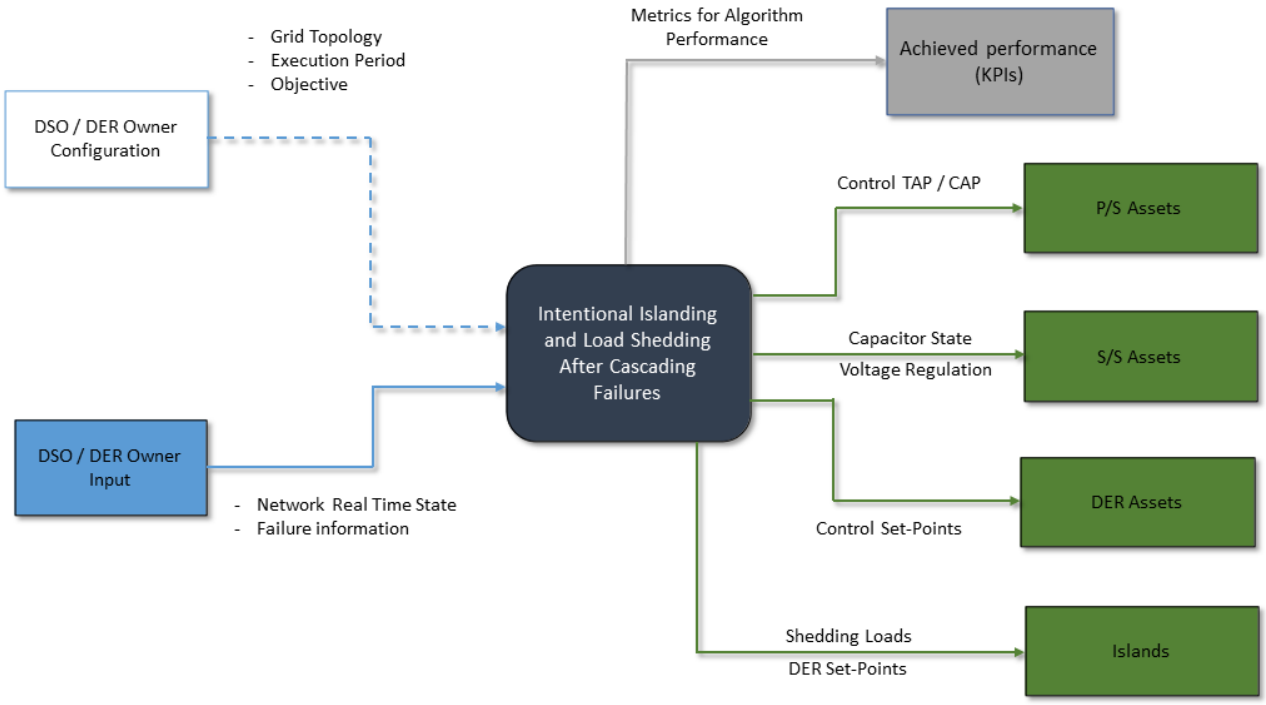

Figure 5-6.1 High-level block-diagram for Islanding algorithm

This project has received funding from the European Union's Horizon 2020 research and innovation programme under grant agreement N°864283

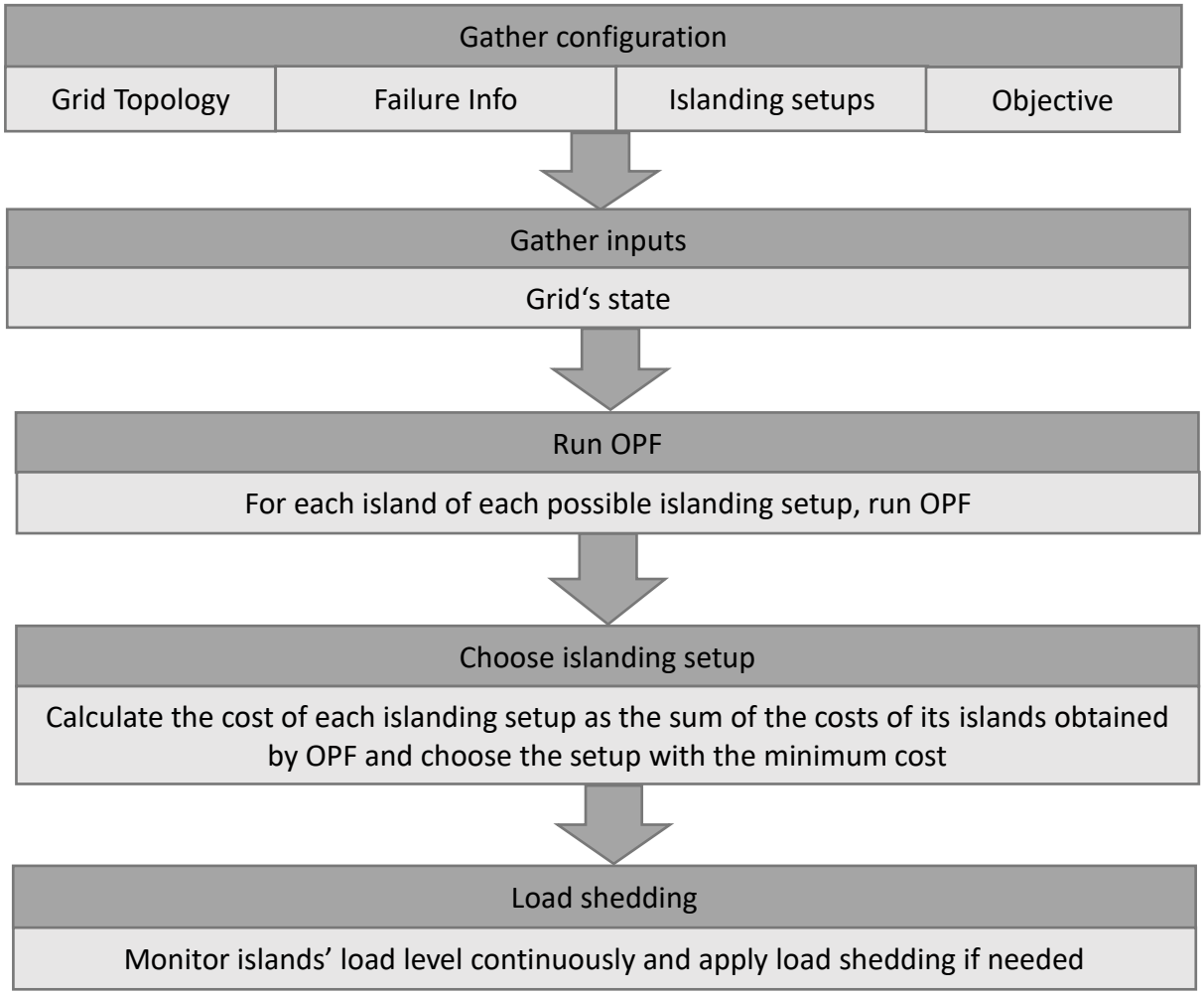

Figure 5-2 Intentional islanding execution process

It has to be mentioned that the OPF is conducted using the software environment presented in 2.3 and is solved by the well-known PSO.

This project has received funding from the European Union's Horizon 2020 research and innovation programme under grant agreement N°864283

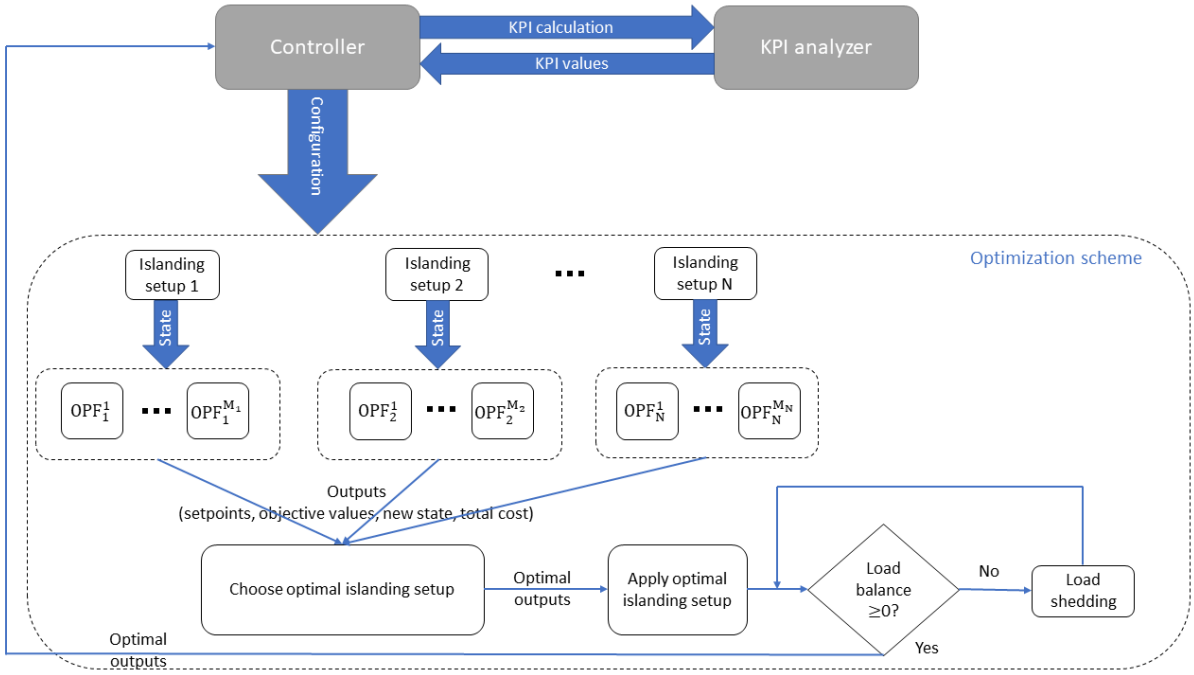

Figure 5-3 Intentional islanding and load shedding scheme

6.4 Demonstration

Apply the scenarios discussed in the Use Case definition document on ebalance-plus Resilience Topology (applied on IN-LAB)
Using the ebalance-plus platform in conjunction with the algorithm is shall be demonstrated that:

a) The algorithm achieves its goals (KPI analysis)

For demonstration purposes, a random case is specified and examined following the steps below.

1) Assumption: All switches are closed except 5, 9, 12, 13, 14 and 15.
2) Specify fault: Failure in lines 5, 6, 12, 16 lead to open switches 3, 4 and 7.
3) Specify all possible islanding setups that are likely to give feasible solutions.
    a. Setup 1: closing switch 5, 12 and 13, 2 islands are formatted as in Figure 5-4.
    b. Setup 2: closing switches 5, 12, 13 and 15, 1 island is formatted as in Figure 5-5.

This project has received funding from the European Union's Horizon 2020 research and innovation programme under grant agreement N°864283

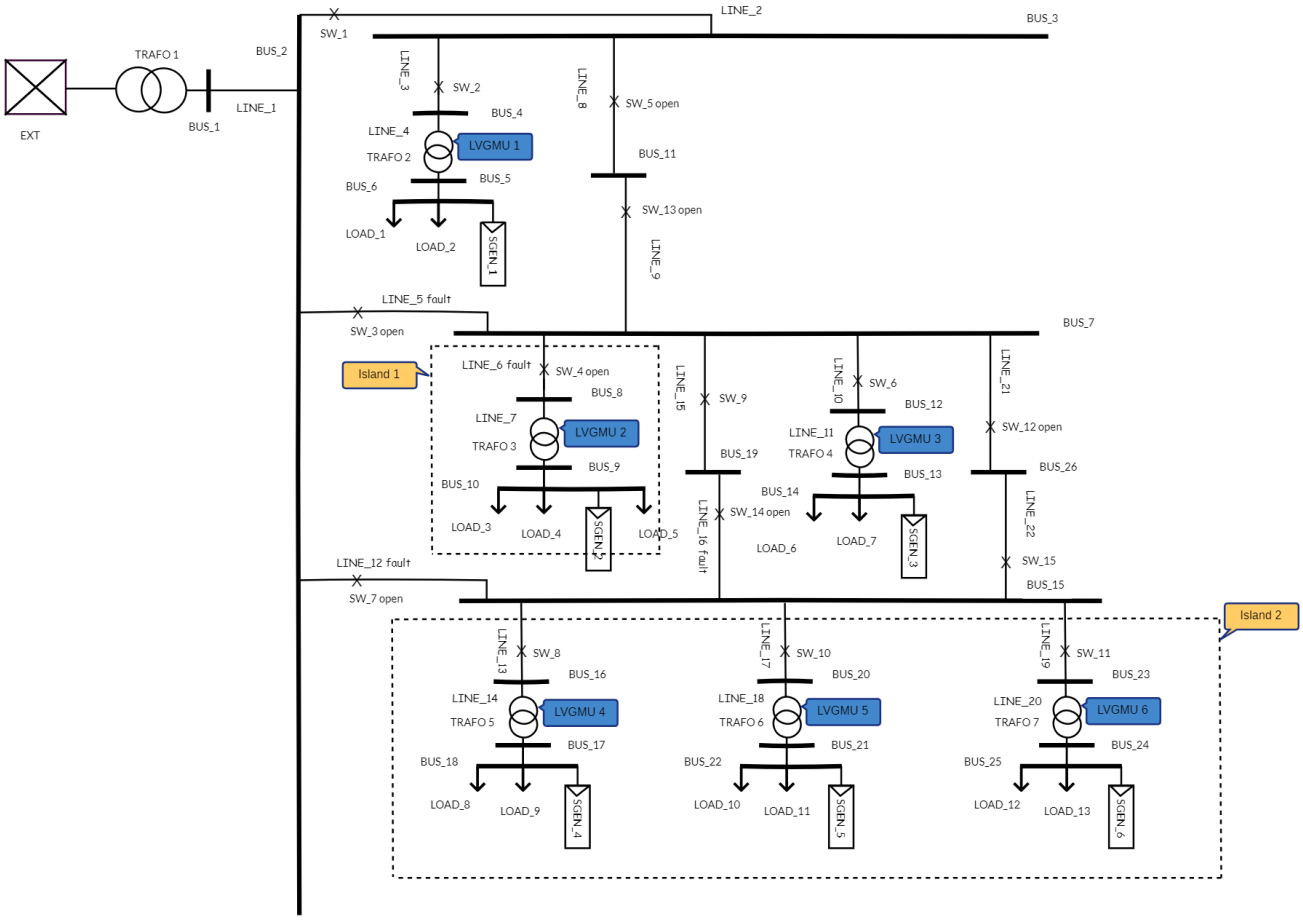

Figure 5-4 Islanding setup 1

This project has received funding from the European Union's Horizon 2020 research and innovation programme under grant agreement N°864283

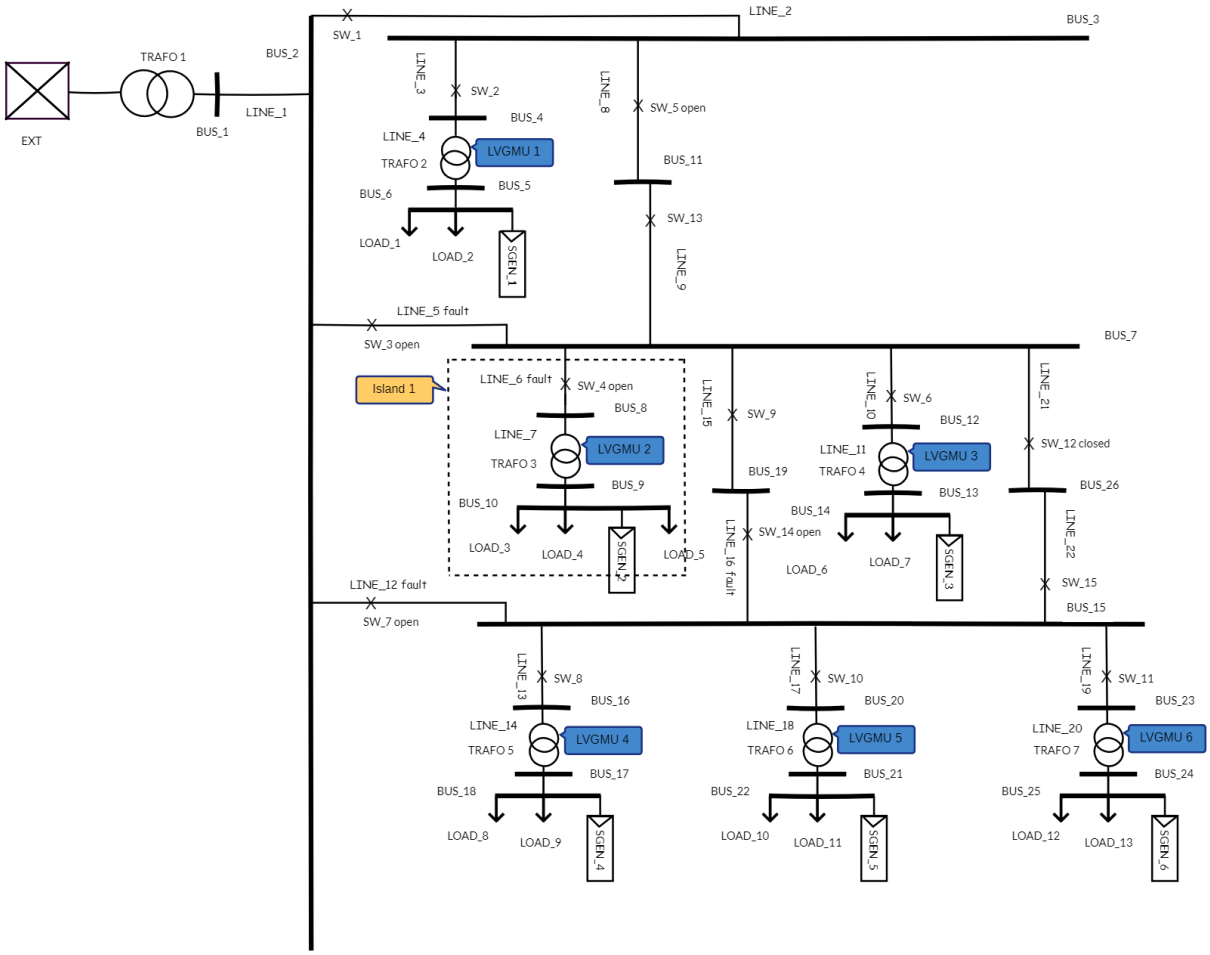

Figure 5-5 Islanding setup 2

4) For each island of each islanding setup, OPF is executed, and a corresponding solution is obtained. In this case, if all solutions are feasible, we obtain 3 solutions S_1^1, S_1^2 Type equation here. S_{11}, S_{12} and $S_2^1 S_{21}$, where the subscripts denote the i-th islanding setup and the superscripts the j-th island of the i-th setup.
5) The cost of each islanding setup is calculated as the sum of the costs of its islands obtained by OPF, i.e. $TC_i = \sum_{j=1}^{N_i} c_j^i$ where TC_i is the total cost of the i-th islanding setup, N_i is the number of islands of the i-th islanding setup and c_j^i is the cost of the j-th island of the i-th islanding setup. The cost is defined as the number of customers served. Here, TC_1 and TC_2 must be calculated. Then, the setup with the minimum cost is chosen.
6) The optimal islanding setup is applied, in the sense of optimal switches configuration.
7) Finally, the load balance of the islands is monitored until the faults have been restored and apply load shedding when needed. The load shedding is conducted following a prioritization of the loads that depends on their size and cruciality.

This project has received funding from the European Union's Horizon 2020 research and innovation programme under grant agreement N°864283

7 LV Transformer status monitoring with PMU & sensors

7.1 State of the art

A transformer faces many different failures. These failures are the result of its operating conditions and its aging and are classified by severity and rate of occurrence. In this context, transformers typically have a maintenance schedule. Most HV and MV transformers are already monitored and maintained consistently since they are expensive assets. LV transformers, on the other hand, are not. As a result, operators do not have visibility in this part of their network for both asset health and network status.

Abnormality in LV transformers can be detected in variations of key parameters. The most important ones refer to temperatures, load current, oil flow and moisture. When a transformer fails, an adverse effect occurs in the continuity of transmission and distribution systems resulting in increase of power system cost and decrease of reliability in electric delivery. As a transformer is a combination of many parts, all of these parts must be checked regularly to maintain the transformer in perfect operating conditions [AD-90].

Based on the above, the use of additional sensors for LV transformers can enhance the capabilities for continuous health monitoring and can enable predictive maintenance functions for these assets [AD-91].

In the context of transformer health, another major advancement for the future of smart grids is the use of Phasor Measurement Unit (PMU) devices. Typical PMU devices have a temporal resolution in the range of 120 measurements per seconds which is very large in relation to traditional SCADA systems that have an acquisition rate between 2 and 4 minutes [AD-94]. The enhanced resolution allows the capture of transient events for voltage and current in a transformer allowing better monitoring and quicker action from operators to prevent faults and increase reliability. Additionally, PMUs are commonly synchronized using a GPS signal or the IEEE 1588 Precision Time Protocol in order to offer detailed data across the network to enhance the capabilities of operators in terms of load balancing.

The data gathered from PMUs can be analyzed in a variety of ways in order to give the desired high-level information to perform predictive maintenance. An approach discussed in [AD-92], mentions the use of the Signal to Noise Ratio (SNR) as a quantitative metric that can demonstrate that a fault is occurring in a transformer. The SNR is derived from the PMU signals and is shown that when a fault starts to manifest in the transformer the SNR band starts to widen and continues to widen as the situation worsens. As such it is argued that this metric can be used as an early warning signal for operators to inspect a potentially faulty transformer.

This project has received funding from the European Union's Horizon 2020 research and innovation programme under grant agreement N°864283

7.2 Scope

In the current scope, the main target is to provide necessary input data to enable predictive maintenance in future iterations. The MUs involved in this use case are the LVGMU and the MVGMU.

The LVGMUs are responsible for generating the desired information. For this to work each LVGMU needs to be equipped with sensors to monitor temperature, vibrations and magnetic field. Additionally, each LVGMU needs to be equipped with a PMU in order to produce the needed high-resolution measurements. Finally, all the participating LVGMUs will be synchronized with GPS clock in order to have synchronized measurements from the PMUs.

The MVGMU will need to collect the information generated from the LVGMUs in order to perform any needed analysis and to produce the desired KPIs. The rate at which this will occur shall be configurable but is dependent on the storage capabilities of the underlying MUs.

7.3 Technical Methodology

As discussed above, the algorithm can be separated in two major components. The data gathering and synchronization on the LVGMU side and the data consolidation and analysis on the MVGMU side. Additionally, it is noted that the LVGMU side also has a retention capability in order to accommodate the high sampling rating of the PMU. This feature is needed in this case since the interaction between the two MUs is not expected to be as frequent as the acquisition rate of the PMU.

The MVGMU side is responsible for propagating the received data to higher level in order to be evaluated individually (in a SCADA system for example). More importantly however, it necessary to enable the calculation of the desired KPIs. Currently two qualitative KPIs have been identified. One concerns the Asset Health Index while the other concerns the Low-Voltage Network Status Stability.

The configuration of the infrastructure is depicted in Figure 7.1.

This project has received funding from the European Union's Horizon 2020 research and innovation programme under grant agreement N°864283

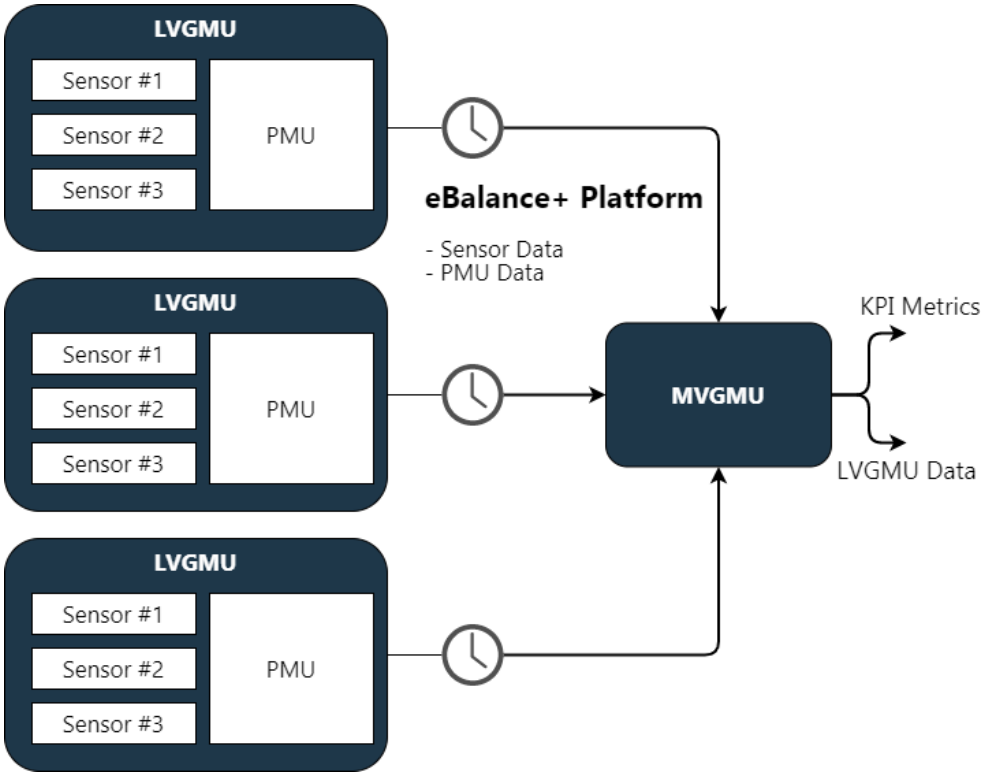

Figure 7.1 Unit Interaction to support PMUs and Sensors

The LVGMU units are responsible for retrieving and propagating data from their PMU and Sensors to the MVGMU unit in a synchronizer manner. The sensors to support the process are for temperature, vibrations and magnetic field. The MVGMU in the end is responsible for gathering the data, calculating the KPIs and other statistical values.

The first KPI is the Asset Health Index. This metric aims to demonstrate the condition of an asset in a scale between 0 and 10. Typically, 0 means that the asset is broken beyond repair while 10 means that the asset is brand new. To calculate the health index multiple values may be used. The most prominent ones as can be seen in [AD-103], [AD-104], refer to the Oil Quality and Age of the asset. In the current context however, a different approach will be used where the three aforementioned sensors (Temperature, Magnetic Field, Vibrations) will be used. This has the benefit that no tampering with the asset is needed in order to install the device. An oil temperature sensor for example would need to be installed inside in a transformer.
Since all the information is dynamic and measured in real time the quality of the asset is calculated in the same manner by taking into account previous readings to determine deterioration of the asset.

The second KPI is the Low Voltage Network Status. This metric aims to demonstrate the voltage quality of the target Asset using the PMU. In that regard, using the PMU measurements it is possible to detect any threshold violations that may occur even in transient states due to the PMU's sampling rate.

Apart from the KPIs themselves, additional statistical measures are provided in order to give an overall picture of the transformer's status. Specifically, statistical analysis is performed in a temporal sense by providing, for example, the average asset temperature per week. Additionally, the spatial analysis is also performed at the MVGMU level by taking into account averages in for all underlying assets.

This project has received funding from the European Union's Horizon 2020 research and innovation programme under grant agreement N°864283

7.4 Demonstration

According to the above, demonstration will focus on constructing meaningful KPIs from the data gathered at the LVGMU level in order to inform the uses of the overall status of each asset. For this particular use-case the topology is not as important.

Instead, demonstration will focus on the creation of profiles of sensor data to examine the KPI values and the statistical evaluations. This is a two-step progress. The first step concerns evaluation on a laboratory environment with simulated data. This aims on the determination and fine tuning of sensor and PMU reading weighting in order to calculate the target KPIs. The second step concerns the application of the approach on a real scenario based on a target demo-site. This is the final validation step of the KPI measurements and the final demonstration of this use-case.

Specifically, effort will be made to simulate / mock various sensor and PMU inputs so as to emulate various use cases. The approach begins with the definition of a nominal scenario where all the readings are within acceptable limits. This will serve as a reference scenario where all the assets are at peak working condition. Based on this reference additional input scenarios will be used to demonstrate the variability of the KPIs as the performance of the assets deteriorates. Additionally, the analysis will help to tune the contribution of each reading in the overall KPI measurement.

All the results, both for the statistics and the KPIs will finally be presented during the deployment on demo-sites for both scenarios.

This project has received funding from the European Union's Horizon 2020 research and innovation programme under grant agreement N°864283

8 Conclusion

The algorithms presented above have been selected with the consideration of multiple common scenarios in the context of reliability and resilience. The rationale is that we want to demonstrate the impact of the ebalance-plus Framework technology in this context by considering and enhancing well-established methodologies.

The ebalance-plus framework primarily provides an approach for decentralized and distributed execution of algorithms and processes to improve modern electrical grids by offering location and communication transparency. The aforementioned algorithms are designed in such a way that maximum benefit from this feature can be achieved.

Especially in the context of reliability and resilience, the framework offers the tremendous benefit of allowing the operation of multiple Management units to achieve a certain goal. For example, in the islanding and the FDIR algorithms, we take advantage of the framework's features by distributing the problem on multiple devices in order to achieve smaller execution time and thus faster results and benefits on the grid. Additionally, by using the framework we can easily understand abnormal situations such as disconnections or any kind of communication loss and thus react accordingly and in new ways to address the problem.

Finally, with the use of the framework we are able to install and interact with more devices even in aspects of the electrical grid that are currently under-maintained. A prime scenario for this is the LV transformers which do not typically have the same monitoring features as their MV or HV counterparts in terms of maintenance. With the use of the ebalance-plus framework and the proposed MUs we can enable robust monitoring approaches by using appropriate sensors and PMU devices in order to monitor them with high fidelity and in a synchronous manner by enabling future technologies such as predictive maintenance.

9 References

[AD-1] Jufri, F.H., Widiputra, V., & Jung, J. (2019). State-of-the-art review on power grid resilience to extreme weather events: Definitions, frameworks, quantitative assessment methodologies, and enhancement strategies.

[AD-2] IPCC, Field CB, Barros V, Stocker TF, Qin D, Dokken DJ, et al. Managing the risks of extreme events and disasters to advance climate change adaptation; 2012. http://doi.org/10.1017/CBO9781139177245.

[AD-3] International Electrotechnical Commission (IEC). IEC glossary: http://std.iec. ch/terms/terms.nsf/0/1036BB0DDCDB80CDC1257E36004BC268? OpenDocument [accessed January 31, 2022].

[AD-4] M. Panteli and P. Mancarella, "The Grid: Stronger, Bigger, Smarter?: Presenting a Conceptual Framework of Power System Resilience," in IEEE Power and Energy Magazine, vol. 13, no. 3, pp. 58-66, May-June 2015.

This project has received funding from the European Union's Horizon 2020 research and innovation programme under grant agreement N°864283

[AD-5] Mar, Adriana & Pereira, Pedro & Martins, João. (2019). A Survey on Power Grid Faults and Their Origins: A Contribution to Improving Power Grid Resilience. Energies. 12. 4667. 10.3390/en12244667.

[AD-6] G. Valverde and T. Van Cutsem, "Model predictive control of voltages in active distribution networks," IEEE Trans. Smart Grid, vol. 4, no. 4, pp. 2152 – 2161, 2013

[AD-7] P. Jahangiri and D. C. Aliprantis, "Distributed Volt/VAr control by PV inverters," *IEEE Trans. Power Syst.*, vol. 28, no. 3, pp. 3429–3439, 2013.

[AD-8] P. Šulc, S. Backhaus, and M. Chertkov, "Optimal distributed control of reactive power via the alternating direction method of multipliers," *IEEE Trans. Energy Convers.*, vol. 29, no. 4, pp. 968–977, 2014.

[AD-9] S. Boyd, "Distributed Optimization and Statistical Learning via the Alternating Direction Method of Multipliers," *Found. Trends® Mach. Learn.*, vol. 3, no. 1, pp. 1–122, 2010.

[AD-10] M. Kraning, E. Chu, J. Lavaei, and S. Boyd, "Message Passing for Dynamic Network Energy Management," *Found. Trends® Optim.*, vol. 1, no. 2, pp. 70–122, 2012.

[AD-11] B. Zhang, A. Y. S. Lam, A. D. Domínguez-García, and D. Tse, "An Optimal and Distributed Method for Voltage Regulation in Power Distribution Systems," *IEEE Trans. Power Syst.*, vol. 30, no. 4, pp. 1714–1726, 2015.

[AD-12] S. Bolognani, R. Carli, G. Cavraro, and S. Zampieri, "Distributed Reactive Power Feedback Control for Voltage Regulation and Loss Minimization," *IEEE Trans. Automat. Contr.*, vol. 60, no. 4, pp. 966–981, 2015.

[AD-13] J. Schiffer, T. Seel, J. Raisch, and T. Sezi, "Voltage Stability and Reactive Power Sharing in Inverter-Based Microgrids with Consensus-Based Distributed Voltage Control," *IEEE Trans. Control Syst. Technol.*, vol. 24, no. 1, pp. 96–109, 2016.

[AD-14] J. W. Simpson-Porco, Q. Shafiee, F. Dorfler, J. C. Vasquez, J. M. Guerrero, and F. Bullo, "Secondary Frequency and Voltage Control of Islanded Microgrids via Distributed Averaging," *IEEE Trans. Ind. Electron.*, vol. 62, no. 11, pp. 7025–7038, 2015.

[AD-15] W. Ren, R. W. Beard, and E. M. Atkins, "Information consensus in multivehicle cooperative control," *IEEE Control Syst. Mag.*, vol. 27, no. 2, pp. 71–82, 2007.

[AD-16] G. Lou, W. Gu, Y. Xu, M. Cheng, and W. Liu, "Distributed MPC-Based Secondary Voltage Control Scheme for Autonomous Droop-Controlled Microgrids," *IEEE Trans. Sustain. Energy*, vol. 8, no. 2, pp. 792–804, 2017.

[AD-17] W. Zheng, W. Wu, B. Zhang, H. Sun, and Y. Liu, "A Fully Distributed Reactive Power Optimization and Control Method for Active Distribution Networks," *IEEE Trans. Smart Grid*, vol. 7, no. 2, pp. 1021–1033, 2016.

[AD-18] C. Feng, Z. Li, M. Shahidehpour, F. Wen, W. Liu, and X. Wang, "Decentralized short-term voltage control in active power distribution systems," *IEEE Trans. Smart Grid*, vol. 9, no. 5, pp. 4566–4576, 2018.

[AD-19] G. Kariniotakis, A. Dimeas, and F. Van Overbeeke (Sections 6.1 6.2), "Pilot Sites: Success Stories and Learnt Lessons," in *Microgrids*, John Wiley & Sons, Ltd, 2013, pp. 206–274.

This project has received funding from the European Union's Horizon 2020 research and innovation programme under grant agreement N°864283

[AD-20] K. E. Antoniadou-Plytaria, I. N. Kouveliotis-Lysikatos, P. S. Georgilakis, and N. D. Hatziargyriou, "Distributed and Decentralized Voltage Control of Smart Distribution Networks: Models, Methods, and Future Research," *IEEE Trans. Smart Grid*, vol. 8, no. 6, pp. 2999–3008, 2017.

[AD-21] H. Markiewicz, A. Klajn, "Voltage Disturbances - Standard EN 50160 - Voltage Characteristics in Public Distribution Systems", *2004 Wroclaw University of Technology*

[AD-22] L. A. Schienbein, J. G. DeSteese, "Distributed Energy Resources, Power Quality and Reliability – Background", *2002 U.S. Department of Energy Office of Power Technologies Office of Distributed Resources*

[AD-23] M. H.J. Bollen, M. Häger, "Power quality: interactions between distributed energy resources, the grid, and other customers"

[AD-24] B. T. Ooi, D. Mcgillis, F. D. Galiana, and R. Marceau, "The Potential of Distributed Generation to Provide Ancillary Services," *2000 Power Eng. Soc. Summer Meet. (Cat. No.00CH37134)*, vol. 00, no. d, pp. 1762–1767, 2000.

[AD-25] G. Lalor, A. Mullane, and M. O'Malley, "Frequency control and wind turbine technologies," *IEEE Trans. Power Syst.*, vol. 20, no. 4, pp. 1905–1913, 2005.

[AD-26] Amund Strømnes Øverjordet, "Synthetic Inertia from Wind Farms - Impacts on Rotor Angle Stability in Existing Synchronous Generators," no. June, 2014.

[AD-27] N. Bhatt et al., "Assessing vulnerability to cascading outages," in 2009 IEEE/PES Power Systems Conference and Exposition, 2009, pp. 1 – 9.

[AD-28] Q. Chen and L. Mili, "Composite Power System Vulnerability Evaluation to Cascading Failures Using Importance Sampling and Antithetic Variates," IEEE Trans. Power Syst., vol. 28, no. 3, pp. 2321 – 2330, Aug. 2013.

[AD-29] Z. Wang, A. Scaglione, and R. J. Thomas, "A Markov-Transition Model for Cascading Failures in Power Grids," in 2012 45th Hawaii International Conference on System Sciences, 2012, pp. 2115 – 2124.

[AD-30] J. Song, E. Cotilla-Sanchez, G. Ghanavati, and P. D. H. Hines, " Dynamic Modeling of Cascading Failure in Power Systems," IEEE Trans. Power Syst., vol. 31, no. 3, pp. 2085 – 2095, May 2016.

[AD-31] Schäfer, B., Witthaut, D., Timme, M. et al. Dynamically induced cascading failures in power grids. Nat Commun 9, 1975 (2018). https://doi.org/10.1038/s41467-018-04287-5

[AD-32] M. H. Athari and Z. Wang, "Stochastic Cascading Failure Model With Uncertain Generation Using Unscented Transform," in IEEE Transactions on Sustainable Energy, vol. 11, no. 2, pp. 1067-1077, April 2020, doi: 10.1109/TSTE.2019.2917842.

[AD-33] W. Ju, K. Sun, and R. Yao, "Simulation of Cascading Outages Using a Power-Flow Model Considering Frequency," IEEE Access, vol. 6, pp. 37784 – 37795, 2018.

[AD-34] P. Pinceti and M. Vanti, "An Algorithm for the Automatic Detection of Islanded Areas Inside an Active Network," in IEEE Transactions on Smart Grid, vol. 6, no. 6, pp. 3020-3028, Nov. 2015, doi: 10.1109/TSG.2015.2414484.

This project has received funding from the European Union's Horizon 2020 research and innovation programme under grant agreement N°864283

[AD-35] Fernández-Porras, P., Panteli, M. and Quirós-Tortós, J. (2018), Intentional controlled islanding: when to island for power system blackout prevention. IET Gener. Transm. Distrib., 12: 3542-3549. https://doi.org/10.1049/iet-gtd.2017.1526

[AD-36] H. Shao and J. Bialek, "When to island in the controlled islanding scheme to prevent imminent wide-area blackouts," 2012 47th International Universities Power Engineering Conference (UPEC), 2012, pp. 1-6, doi: 10.1109/UPEC.2012.6398544.

[AD-37] D. N. Trakas, E. M. Voumvoulakis and N. D. Hatziargyriou, "Controlled islanding of power networks using machine learning algorithm," MedPower 2014, 2014, pp. 1-6, doi: 10.1049/cp.2014.1683.

[AD-38] Abokhalil, A.G.; Awan, A.B.; Al-Qawasmi, A.-R. Comparative Study of Passive and Active Islanding Detection Methods for PV Grid-Connected Systems. Sustainability 2018, 10, 1798. https://doi.org/10.3390/su10061798

[AD-39] A. Timbus, A. Oudalov and C. N. M. Ho, "Islanding detection in smart grids," 2010 IEEE Energy Conversion Congress and Exposition, 2010, pp. 3631-3637, doi: 10.1109/ECCE.2010.5618306.

[AD-40] Loiy Rashed Almobasher , Ibrahim Omar A Habiballah, 2020, Review of Power System Faults, INTERNATIONAL JOURNAL OF ENGINEERING RESEARCH & TECHNOLOGY (IJERT) Volume 09, Issue 11 (November 2020),

[AD-41] Bunnoon, Pituk. "Fault Detection Approaches to Power System: State-of-the-Art Article Reviews for Searching a New Approach in the Future." International Journal of Electrical and Computer Engineering 3 (2013): 553-560.

[AD-42] P. Linares and L. Rey, "The costs of electricity interruptions in Spain. Are we sending the right signals?" Energy Policy, vol. 61, pp. 751–760, Oct. 2013.

[AD-43] M. Kezunovic, "Smart fault location for smart grids," IEEE Trans. Smart Grid, vol. 2, no. 1, pp. 11–22, Mar. 2011.

[AD-44] A. Zidan et al., "Fault Detection, Isolation, and Service Restoration in Distribution Systems: State-of-the-Art and Future Trends," in IEEE Transactions on Smart Grid, vol. 8, no. 5, pp. 2170-2185, Sept. 2017, doi: 10.1109/TSG.2016.2517620.

[AD-45] P. V. Dahiwale and N. M. Pindoriya, "Review on Fault Management in Hybrid Microgrid," 2019 IEEE Region 10 Symposium (TENSYMP), 2019, pp. 415-422, doi: 10.1109/TENSYMP46218.2019.8971122.

[AD-46] D. Fan, Y. Ren, Q. Feng, Y. Liu, Z. Wang and J. Lin, "Restoration of smart grids: Current status challenges and opportunities", Renew. Sustain. Energy Rev., vol. 143, Jun. 2021.

[AD-47] A. Zidan and E. F. El-Saadany, "A cooperative multiagent frame- work for self-healing mechanisms in distribution systems," IEEE Trans. Smart Grid, vol. 3, no. 3, pp. 1525–1539, Sep. 2012.

[AD-48] A. Skoonpong and S. Sirisumrannukul, "Network reconfiguration for reliability worth enhancement in distribution systems by simulated annealing," in Proc. 5th Int. Conf. Elect. Eng./Electron. Comput. Telecommun. Inf. Technol., Krabi, Thailand, May 2008, pp. 937–940.

This project has received funding from the European Union's Horizon 2020 research and innovation programme under grant agreement N°864283

[AD-49] M. A. Shahin, "Smart grid self-healing implementation for underground distribution networks," in Proc. IEEE Innov. Smart Grid Technol. Conf., Bengaluru, India, Nov. 2013, pp. 1 – 5.

[AD-50] M. A. Shahin, "Smart grid self-healing implementation for underground distribution networks," in Proc. IEEE Innov. Smart Grid Technol. Conf., Bengaluru, India, Nov. 2013, pp. 1 – 5.

[AD-51] E. Coster, W. Kerstens, and T. Berry, "Self healing distribution networks using smart controllers," in Proc. 22nd Int. Conf. Exhibit. Elect. Distrib. (CIRED), Stockholm, Sweden, Jun. 2013, pp. 1 – 4.

[AD-52] A. Varžiû, K. Slivariû, and M. Šporec, "Detecting faults in MV net- work using GPRS," in Proc. 22nd Int. Conf. Elect. Distrib., Stockholm, Sweden, Jun. 2013, pp. 1 – 3.

[AD-53] D. T. Brown and A. L. Gielink. (Feb. 2015). A Utility's Experience in the Implementation of Substation Automation Projects. [Online]. Available: https://www.gedigitalenergy.com/ smartgrid/Dec07/5-substation_automation.pdf

[AD-54] A. Zidan and E. F. El-Saadany, "Incorporating load variation and variable wind generation in service restoration plans for distribution systems," Energy, vol. 57, pp. 682 – 691, Aug. 2013.

[AD-55] J. Vasco, R. Ramlachan, J. Wong, and L. Wang, "An automated fault location system as a decision support tool for system operators," in Proc. 61st Annu. Conf. Protective Relay Eng., College Station, TX, USA, Apr. 2008, pp. 556 – 572.

[AD-56] M. Kezunovic, "Smart fault location for smart grids," IEEE Trans. Smart Grid, vol. 2, no. 1, pp. 11 – 22, Mar. 2011.

[AD-57] G. D. Ferreira et al., "Impedance-based fault location for overhead and underground distribution systems," in Proc. North Amer. Power Symp., Champaign, IL, USA, Sep. 2012, pp. 1 – 6.

[AD-58] M.-S. Choi, S.-J. Lee, S.-I. Lim, D.-S. Lee, and X. Yang, "A direct three-phase circuit analysis-based fault location for line-to-line fault," IEEE Trans. Power Del., vol. 22, no. 4, pp. 2541 – 2547, Oct. 2007.

[AD-59] J. C. S. Souza, M. A. P. Rodrigues, M. T. Schilling, and M. B. D. C. Filho, "Fault location in electrical power systems using intelligent systems techniques," IEEE Trans. Power Del., vol. 16, no. 1, pp. 59 – 67, Jan. 2001.

[AD-60] C. Y. Teo and H. B. Gooi, "Artificial intelligence in diagnosis and supply restoration for a distribution network," IEE Proc. Gener. Transm. Distrib., vol. 145, no. 4, pp. 444 – 450, Jul. 1998.

[AD-61] J. A. Momoh, L. G. Dias, and D. N. Laird, "An implementation of a hybrid intelligent tool for distribution system fault diagnosis," IEEE Trans. Power Del., vol. 12, no. 2, pp. 1035 – 1040, Apr. 1997.

[AD-62] S. Lin, Z. Y. He, X. P. Li, and Q. Q. Qian, "Travelling wave time-frequency characteristic-based fault location method for transmis- sion lines," IET Gener., Transm. Distrib., vol. 6, no. 8, pp. 764 – 772, Aug. 2012.

This project has received funding from the European Union's Horizon 2020 research and innovation programme under grant agreement N°864283

[AD-63] M. Pourahmadi-Nakhli and A. A. Safavi, "Path characteristic frequency-based fault locating in radial distribution systems using wavelets and neural networks," IEEE Trans. Power Del., vol. 26, no. 2, pp. 772 – 781, Apr. 2011.

[AD-64] J. Sadeh, E. Bakhshizadeh, and R. Kazemzadeh, "A new fault location algorithm for radial distribution systems using modal analysis," Int. J. Elect. Power Energy Syst., vol. 45, no. 1, pp. 271 – 278, Feb. 2013.

[AD-65] Personal, E., Garcia, A., Parejo, A., Larios, D.F., Biscarri, F., & León, C. (2016). A Comparison of Impedance-Based Fault Location Methods for Power Underground Distribution Systems. Energies, 9, 1022.

[AD-66] L. Andrade,T. Ponce de Leao,Travelling Wave Based Fault Location Analysis for Transmission Lines, EPJ Web of Conferences, vol.33(2012)04005, https://doi.org/10.1051/epjconf/20123304005

[AD-67] T. Ghanbari and E. Farjah, "A multiagent-based fault-current limiting scheme for the microgrids," IEEE Trans. Power Del., vol. 29, no. 2, pp. 525 – 533, Apr. 2014.

[AD-68] L. Whei-Min and C. Hong-Chan, "A new approach for distribution feeder reconfiguration for loss reduction and service restoration," IEEE Trans. Power Del., vol. 13, no. 3, pp. 870 – 875, Jul. 1998.

[AD-69] S. P. Singh, G. S. Raju, G. K. Rao, and M. Afsari, "A heuristic method for feeder reconfiguration and service restoration in distribu- tion networks," Int. J. Elect. Power Energy Syst., vol. 31, nos. 7 – 8, pp. 309 – 314, Sep. 2009.

[AD-70] M. R. Kleinberg, K. Miu, and H.-D. Chiang, "Improving service restoration of power distribution systems through load curtailment of in-service customers," IEEE Trans. Power Syst., vol. 26, no. 3, pp. 1110 – 1117, Aug. 2011.

[AD-71] D. Shirmohammadi, "Service restoration in distribution networks via network reconfiguration," IEEE Trans. Power Del., vol. 7, no. 2, pp. 952 – 958, Apr. 1992.

[AD-72] M.-S. Tsai, "Development of an object-oriented service restoration expert system with load variations," IEEE Trans. Power Syst., vol. 23, no. 1, pp. 219 – 225, Feb. 2008.

[AD-73] S. Srivastava and K. L. Butler-Burry, "Expert-system method for auto-matic reconfiguration for restoration of shipboard power systems," IEE Proc. Gener., Transm. Distrib., vol. 153, no. 3, pp. 253 – 260, May 2006.

[AD-74] S. J. Lee, K. H. Kim, H. Y. Kim, J. K. Lee, and K. Y. Nam, "Expert system-aided service restoration in distribution automation", in Proc. IEEE Int. Conf. Syst. Man Cybern., vol. 1. Chicago, IL, USA, Oct. 1992, pp. 157 – 161.

[AD-75] K. Manjunath and M. R. Mohan, "A new hybrid multi-objective quick service restoration technique for electric power distribution systems," Int. J. Elect. Power Energy Syst., vol. 29, no. 1, pp. 51 – 64, Jan. 2007.

[AD-76] Y. Kumar, B. Das, and J. Sharma, "Multiobjective, multiconstraint service restoration of electric power distribution system with prior- ity

This project has received funding from the European Union's Horizon 2020 research and innovation programme under grant agreement N°864283

customers," IEEE Trans. Power Del., vol. 23, no. 1, pp. 261 – 270, Jan. 2008.

[AD-77] Y. Jiang, J. Jiang, and Y. Zhang, "A novel fuzzy multiobjective model using adaptive genetic algorithm based on cloud theory for service restoration of shipboard power systems," IEEE Trans. Power Syst., vol. 27, no. 2, pp. 612 – 620, May 2012.

[AD-78] S. Khushalani, J. M. Solanki, and N. N. Schulz, "Optimized restoration of unbalanced distribution systems," IEEE Trans. Power Syst., vol. 22, no. 2, pp. 624 – 630, May 2007.

[AD-79] R. M. Ciric and D. S. Popovic, "Multi-objective distribution network restoration using heuristic approach and mix integer programming method," Int. J. Elect. Power Energy Syst., vol. 22, no. 7, pp. 497 – 505, Oct. 2000.

[AD-80] S. R. Islam, K. M. Muttaqi, and D. Sutanto, "A decentralized multiagent-based voltage control for catastrophic disturbances in a power system, " IEEE Trans. Ind. Appl., vol. 51, no. 2, pp. 1201 – 1214, Mar./Apr. 2015.

[AD-81] A. Vaccaro, V. Loia, G. Formato, P. Wall, and V. Terzija, "A self-organizing architecture for decentralized smart microgrids synchroniza-tion, control, and monitoring," IEEE Trans. Ind. Informat., vol. 11, no. 1, pp. 289 – 298, Feb. 2015.

[AD-82] M. Shafie-Khah and J. P. S. Catalao, "A stochastic multi-layer agent-based model to study electricity market participants behavior," IEEE Trans. Power Syst., vol. 30, no. 2, pp. 867 – 881, Mar. 2015.

[AD-83] T. Khalifa, K. Naik, and A. Nayak, "A survey of communication proto-cols for automatic meter reading applications," IEEE Commun. Surveys Tuts., vol. 13, no. 2, pp. 168 – 182, Jun. 2011.

[AD-84] The role of communication systems in smart grids: Architectures, technical solutions and research challenges

[AD-85] Smart grid sensor data collection, communication, and networking: A tutorial

[AD-86] Z. Wang and J. Wang, "Self-healing resilient distribution systems based on sectionalization into microgrids," IEEE Trans. Power Syst., vol. 30, no. 6, pp. 3139 – 3149, Nov. 2015.

[AD-87] S. A. Arefifar, Y. A.-R. I. Mohamed, and T. El-Fouly, "Optimized multiple microgrid-based clustering of active distribution systems con-sidering communication and control requirements," IEEE Trans. Ind. Electron., vol. 62, no. 2, pp. 711 – 723, Feb. 2015.

[AD-88] Z. Wang, B. Chen, J. Wang, and C. Chen, "Networked microgrids for self-healing power systems," IEEE Trans. Smart Grid, vol. 7, no. 1, pp. 310 – 319, Jan. 2016.

[AD-89] D. S. Sanches, J. B. A. London, Jr., and A. C. B. Delbem, "Multi-objective evolutionary algorithm for single and multiple fault service restoration in large-scale distribution systems," Elect. Power Syst. Res., vol. 110, pp. 144 – 153, May 2014.

[AD-90] Priyanka R, Chaithrashree N, Sangeetha S, Bhagyalakshmi, Divyashree A, "Design and Implementation of Real-Time Transformer Health

This project has received funding from the European Union's Horizon 2020 research and innovation programme under grant agreement N°864283

Monitoring System using Raspberry-Pi", International Journal of Engineering Research & Technology (IJERT), 2018

[AD-91] Farzana Kabir, Brandon Foggo, Nanpeng Yu, "Data Driven Predictive Maintenance of Distribution Transformers", 2018 China International Conference on Electricity Distribution (CICED 2018)

[AD-92] Shazmina Jamil, Aehtsham-Ul-Haq, "Analysis of Health of Transformer using Different Loading Conditions", International Journal of Engineering Works, Vol. 8, Issue 01, PP. 31-36, January 2021

[AD-93] Daisuke Kato, Hiroo Horii, Taichiro Kawahara, "Next-generation SCADA/EMS Designed for Large Penetration of Renewable Energy", Hitachi Review Vol. 63 (2014), No. 4

[AD-94] https://en.wikipedia.org/wiki/Phasor_measurement_unit
Last Access: 11/30/2021

[AD-95] L. Thurner, A. Scheidler, A. Probst, and M. Braun, "Heuristic optimization for network restoration and expansion in compliance with the single contingency policy," IET Generation, Transmission & Distribution, vol. 11, pp. 4264 – 4273, July 2017.

[AD-96] A. Scheidler, L. Thurner, and M. Braun, "Heuristic optimisation for automated distribution system planning in network integration studies," IET Renewable Power Generation, vol. 12, no. 5, pp. 530 – 538, April 2018

[AD-97] J.-H. Menke, J. Hegemann, S. Gehler, and M. Braun, "Heuristic monitoring method for sparsely measured distribution grids," International Journal of Electrical Power & Energy Systems, vol. 95, pp. 146 – 155, 2018.

[AD-98] H. Wang, M. Kraiczy, S. Wende-von Berg et al., "Reactive power coordination on strategies with distributed generators in distribution networks," in 1st International Conference on Large-Scale Grid Integration of Renewable Energy in India, September 2017

[AD-99] J. Kennedy and R. Eberhart, "Particle swarm optimization," in Proceedings of ICNN'95 - International Conference on Neural Networks, vol. 4, pp. 1942 – 1948.

[AD-100] Y. del Valle, G. K. Venayagamoorthy, S. Mohagheghi, J. C. Hernandez, and R. G. Harley, "Particle swarm optimization: Basic concepts, variants and applications in power systems," IEEE Transactions on Evolutionary Computation. 2008.

[AD-101] Y. Shi and R. Eberhart, "Modified particle swarm optimizer," in Proceedings of the IEEE Conference on Evolutionary Computation, ICEC, 1998.

[AD-102] F. Marini and B. Walczak, "Particle swarm optimization (PSO). A tutorial," Chemom. Intell. Lab. Syst., vol. 149, pp. 153 – 165, Dec. 2015.

[AD-103] https://www.tdworld.com/test-and-measurement/article/20972278/building-a-transformer-health-index

[AD-104] Dr R.J Heywood and Dr T. McGrail, "Generating Asset Health Indices Which Are Useful and Auditable"

This project has received funding from the European Union's Horizon 2020 research and innovation programme under grant agreement N°864283